Optimal designs of the Exponentially Weighted Moving Average (EWMA) median chart for known and estimated parameters based on median run length

Z. Chong, K. Tan, Michael Khoo, W. Teoh, P. Castagliola

Optimal designs of the Exponentially Weighted Moving Average (EWMA) median chart for known and estimated parameters based on median run length

Z. L. Chong (Corresponding author)
School of Mathematical Sciences,
Universiti Sains Malaysia, 11800 Penang, Malaysia
chongzl@usm.my

K. L. Tan
Department of Physical and Mathematical Science, Faculty of Science,
Universiti Tunku Abdul Rahman, 31900 Kampar, Perak, Malaysia
skyleong911@gmail.com

Michael B. C. Khoo
School of Mathematical Sciences,
Universiti Sains Malaysia, 11800 Penang, Malaysia
mkbc@usm.my

W. L. Teoh
School of Mathematical and Computer Sciences,
Heriot-Watt University Malaysia,
62200 Putrajaya, Malaysia
wei_lin.teoh@hw.ac.uk

P. Castagliola
Université de Nantes & LS2N UMR 6004, Nantes, France
philippe.castagliola@univ-nantes.fr

Optimal designs of the Exponentially Weighted Moving Average (EWMA) median chart for known and estimated parameters based on median run length

In the literature, the sole dependence on the ARL as the performance measure of a control chart has received much criticism. This is because interpretation based on the ARL alone can be misleading, as the shape and skewness of the run-length distribution vary according to the magnitude of the process mean shift. Therefore, we consider the median run length (MRL) performance measure for optimal EWMA median chart when process parameters are known and estimated. We provide an illustrative example to show the application of the optimal EWMA median chart based on expected median run length (EMRL).

Keywords: Estimated parameters; exponentially weighted moving average (EWMA) median chart; known parameters; median run length (MRL); steady-state; zero-state.

1. Introduction

Quality is an essential component considered by consumers in choosing among various services or products. Hence, it is important for all industries to offer quality services or manufacture quality products so that they can remain competitive against their competitors. For instance, by having a process that manufactures quality products, the manufacturing company will have a good production yield, low production cost and products that can exceed the customers' expectations. There are no service operations or production processes that can remain stable forever. Statistical Process Control (SPC) is a collection of powerful tools that applies statistical techniques to minimize the variability and provide continuous quality improvement of a process. SPC is widely used in service and industrial sectors. Control chart is one of the most important SPC tools to maintain, as well as improve the quality of services and products. Control chart enables practitioners to examine whether the quality characteristics of their products are in-control

(IC), i.e. within the chart's control limits. In this competitive era, control chart should be simple to construct, interpret, implement and able to detect small and large shifts in the process mean efficiently.

The Shewhart mean ($\bar{X}$) chart is one of the most well-known control chart to date because of its simplicity. However, the $\bar{X}$ chart requires the assumption that the process follows a normal distribution to be satisfied as it uses sample average in process monitoring, which is easily affected by outliers and leads to a high level of out-of-control (OOC) signal. To alleviate this problem, Janacek and Meikle (1997) suggested the median ($\tilde{X}$) chart. Although the $\bar{X}$ chart is more effective compared to the $\tilde{X}$ chart, Khoo (2005) stated that the $\tilde{X}$ chart is a good substitute for the $\bar{X}$ chart as it is more robust against outliers. In practice, the $\tilde{X}$ chart is preferred due to its robustness against contamination, outliers and small deviations from normality. It is worth mentioning that Statistical Process Control (SPC) charts are designed to mainly detect permanent shifts and not occasional disturbances (like outliers). When a permanent shift happens, it will remain there until the assignable causes have been removed. On the other hand, outliers are disturbances that happen occasionally and they are usually not associated with any assignable cause, instead they are due to other causes such as careless mistakes in recording.

In addition, it is well-known that the Shewhart $\bar{X}$ chart is effective in detecting large process shifts. However, it is less sensitive to small and moderate process mean shifts as it is a memoryless-type control chart. A memoryless control chart is a control procedure for which the decision is based on the current observation only, which makes the control chart relatively insensitive to small and moderate mean shifts. Therefore, various memory-type control charts are proposed to enhance the performance of the Shewhart $\bar{X}$ chart towards detecting small and moderate process mean shifts. The memory-type control charts are designed to incorporate past and present information in order

to obtain a better performance in the detection of small and moderate process mean shifts compared to the memoryless-type control charts which ignore past information (Abbas, Riaz, and Does 2013). The most commonly used memory-type control charts are the cumulative sum (CUSUM) and exponentially weighted moving average (EWMA) charts proposed by Page (1954) and Roberts (1959), respectively.

Roberts (1959) proposed the EWMA $\bar{X}$ chart and it has attracted the interest of many researchers, see, for example, Simoes, Epprecht, and Costa (2010), Eleftheriou and Farmakis (2016), Shamsuzzaman et al. (2016) and Zwetsloot, Schoonhoven, and Does (2016). This is because the EWMA $\bar{X}$ chart can detect small and moderate shifts in the process mean effectively. Moreover, this may be due to the fact that many researchers considered the EWMA $\bar{X}$ chart to be robust against deviations from the normality assumption. However, Human, Kritzinger, and Chakraborti (2011) proved that this consideration is invalid, especially when using the EWMA $\bar{X}$ chart to monitor contaminated data. Castagliola (2001) noted that the EWMA $\tilde{X}$ chart is a suitable alternative to the EWMA $\bar{X}$ chart as median is less affected by deviations from the normality assumption compared to the mean. Since then, various types of median control charts were proposed, see, for instance, the $\tilde{X}$ chart for the detection of permanent mean shifts (Khoo, 2005), generally weighted moving average (GWMA) $\tilde{X}$ chart (Sheu and Yang 2006) and CUSUM $\tilde{X}$ chart (Yang, Pai, and Wang 2010).

Surprisingly, we observe that all the $\tilde{X}$ charts in the current literature are designed based on the average run length (ARL) performance metric. Here, the ARL is defined as the average number of sample points that need to be plotted on a chart before the chart issues an OOC signal. However, many researchers have criticized the use of the ARL as the sole performance metric of a control chart, see, for example, Bischak and Trietsch (2007), Teh et al. (2015), Khoo et al. (2015), Lee

and Khoo (2017), and Tang et al. (2019a). The main critique of using the ARL alone to characterize the whole run-length (RL) distribution is that the RL distribution is known to be highly right-skewed for an IC process or a process with small mean shifts (Gan, 1993). To solve this problem, many researchers suggested the use of the percentiles of the RL distribution to characterize the whole RL distribution for various control charts, see, for example, the EWMA $\bar{X}$ chart (Jones, Champ, and Rigdon 2001), CUSUM $\bar{X}$ chart (Jones, Champ, and Rigdon 2004), Shewhart $\bar{X}$ chart (Chakraborti 2007), synthetic $\bar{X}$ chart (Khoo et al. 2012), among others.

Among the different percentiles of the RL distribution, many researchers such as Khoo et al. (2011), Low et al. (2012), Teoh et al. (2014), and Lee and Khoo (2017) demonstrated that the 50th percentile of the RL distribution, also known as the median run length (MRL), is a better performance measure compared to the ARL, regardless of the type of control charts. This is because the MRL is less affected by the skewness of the RL distribution and gives a better measure of central tendency compared to the ARL (Maravelakis, Panaretos, and Psarakis 2005). Moreover, in practical applications, it is common that there is a lack of historical data to determine the actual shift size or in many situations, the shift size varies based on some unknown stochastic models. To tackle this problem, we suggest the use of expected MRL (EMRL) as the performance metric of a chart when the shift size is unknown. Note that the EMRL performance measure is obtained by integrating over the density function $f_\delta(\delta)$ for a range of shift sizes from $\delta_{\min}$ to $\delta_{\max}$, where $\delta_{\min}$ and $\delta_{\max}$ denote the lower and upper bounds of the shift sizes, respectively. The EMRL performance measure was also considered by Teoh et al. (2017), Tang et al. (2019a), and Lim et al. (2019), among others.

Most of the control charts discussed earlier are designed by assuming that the process parameters are known (Case-K) or can be accurately estimated from the Phase-I samples. However,

in various practical situations, the process parameters, i.e. the mean and the variance are usually unknown (Case-U) and need to be estimated from a finite number of Phase-I samples. It is worth mentioning that the performance of control charts deteriorates significantly if the Case-K assumption is invalid, due to the variability in estimating the parameters. Recently, many researchers have investigated various control charts under the Case-U scenario, see for example, Zwetsloot and Woodall (2017), Chong et al. (2019, 2020), Tang et al. (2019a, 2019b) and Hu et al. (2019). Interested readers are referred to Jensen et al. (2006) and Psarakis, Vyniou, and Castagliola (2014) for literature review of Case-U control charts.

Due to the advantages of the MRL and EMRL performance metrics, in this article, we investigate the optimal designs of the Case-K EWMA $\tilde{X}$ chart by minimizing the OOC MRL and EMRL, for both the known and unknown shift size cases, respectively. Moreover, all the $\tilde{X}$ charts in the current literature are designed to investigate the zero-state performance, where it is assumed that the Phase-II process being monitored starts out-of-control. However, in practical situations, we cannot ignore the steady-state performance, where it is assumed that for the Phase II process monitoring, the process remains in the IC state for a long duration of time before the process goes OOC. Hence, we investigate both the zero- and steady-state Case-K performances of the EWMA $\tilde{X}$ chart in this article. Moreover, we evaluate the performances of the optimal EWMA $\tilde{X}$ chart under Case-U situations.

This article is structured into several sections as follows: The plotting statistic and some characteristics of the EWMA $\tilde{X}$ chart are discussed in Sections 2 and 3 for known and unknown process parameters, respectively. The performance of the Case-K EWMA $\tilde{X}$ chart, in terms of the ARL, SDRL and percentiles of the RL distribution is given in Section 4. In Section 5, the optimization designs of the EWMA $\tilde{X}$ chart using the MRL and EMRL performance metrics are

provided. Section 6 compares the EWMA $\tilde{X}$ and Shewhart $\tilde{X}$ charts when the shift size is either known or unknown. Section 6 also discusses the effect of parameters estimation on the performance of the EWMA $\tilde{X}$ chart. The application of the EWMA $\tilde{X}$ chart is illustrated using a real industrial dataset in Section 7. Some concluding remarks are given in Section 8.

2. The EWMA $\tilde{X}$ chart when parameters are known

Assume that samples $\{Y_{i,1}, Y_{i,2}, \ldots, Y_{i,n}\}$, for $i \in 1, 2, \ldots$, are taken from n independent and identically distributed normal random variables, i.e. $N(\mu_0 + \delta\sigma_0, \sigma_0^2)$, where μ_0 and σ_0 are the IC process mean and standard deviation, respectively, and δ is the size of the standardized mean shift. Let $\tilde{Y}_i$ represents the sample median of the i^{th} sample, i.e.

$$\tilde{Y}_i = \begin{cases} Y_{i,\left(\frac{n+1}{2}\right)}, & \text{if } n \text{ is odd} \\ \frac{Y_{i,\left(\frac{n}{2}\right)} + Y_{i,\left(\frac{n}{2}+1\right)}}{2}, & \text{if } n \text{ is even} \end{cases}, \tag{1}$$

where $\{Y_{i,(1)}, Y_{i,(2)}, \ldots, Y_{i,(n)}\}$ are the measurements of the i^{th} sample arranged in ascending order. For ease of implementation of median-type charts, in practice, odd n is usually considered. This is because the computation of the sample median is faster and easier, when n is an odd value. Therefore, in this article, we will only consider the cases where n is an odd value. The Case-K EWMA $\tilde{X}$ chart's plotting statistic for the i^{th} sample is given as

$$Z_i = (1 - \lambda)Z_{i-1} + \lambda\tilde{Y}_i, \tag{2}$$

where $\lambda \in (0,1]$ is a smoothing constant and $Z_0 = \mu_0$. The upper control limit (UCL) and lower control limit (LCL) of the Case-K EWMA $\tilde{X}$ chart are calculated as

$$UCL = \mu_0 + K\sigma_0 \tag{3a}$$

and

$$LCL = \mu_0 - K\sigma_0, \tag{3b}$$

respectively, where K is a positive constant.

We model the RL characteristics of the Case-K EWMA $\tilde{X}$ chart using the Markov chain method. Note that we apply the Markov chain model introduced by Brook and Evans (1972), which divides the interval between the lower and upper control limits into $2u+1$ subintervals $(H_j - \Delta, H_j + \Delta]$, for $j \in \{-u, \ldots, 0, \ldots, +u\}$, each centered at $H_j = \frac{LCL+UCL}{2} + 2j\Delta$, where $2\Delta = \frac{UCL-LCL}{2u+1}$ (see Figure 1). Every subinterval $(H_j - \Delta, H_j + \Delta]$, for $j \in \{-u, \ldots, 0, \ldots, +u\}$ denotes a transient state of the Markov chain. The Markov chain is considered as in the transient state $j \in \{-u, \ldots, 0, \ldots, +u\}$ at sample i if $Z_i \in (H_j - \Delta, H_j + \Delta]$, otherwise, the Markov chain reaches the absorbing state $(-\infty, LCL] \cup [UCL, +\infty)$. The transition probability matrix (tpm) $\mathbf{P}$ which is used to model the RL characteristics of the Case-K EWMA $\tilde{X}$ chart is (Lucas and Saccucci, 1990)

$$\mathbf{P} = \begin{pmatrix} \mathbf{R} & \mathbf{r} \\ \mathbf{0}^T & 1 \end{pmatrix}, \tag{4}$$

where $\mathbf{r} = \mathbf{1} - \mathbf{R1}$ with $\mathbf{1} = (1, 1, \ldots, 1)^T$ and $\mathbf{0} = (0, 0, \ldots, 0)^T$. Here, $\mathbf{R}$ is a submatrix of size $(2u+1, 2u+1)$ containing the probabilities $R_{j,k}$, which are associated with the $2u+1$ transient states defined earlier, i.e.

$$\mathbf{R} = \begin{bmatrix} R_{-u,-u} & \cdots & R_{-u,-1} & R_{-u,0} & R_{-u,+1} & \cdots & R_{-u,+u} \\ \vdots & \vdots & \vdots & \vdots & \vdots & \vdots & \vdots \\ R_{-1,-u} & \cdots & R_{-1,-1} & R_{-1,0} & R_{-1,+1} & \cdots & R_{-1,+u} \\ R_{0,-u} & \cdots & R_{0,-1} & R_{0,0} & R_{0,+1} & \cdots & R_{0,+u} \\ R_{+1,-u} & \cdots & R_{+1,-1} & R_{+1,0} & R_{+1,+1} & \cdots & R_{+1,+u} \\ \vdots & \vdots & \vdots & \vdots & \vdots & \vdots & \vdots \\ R_{+u,-u} & \cdots & R_{+u,-1} & R_{+u,0} & R_{+u,+1} & \cdots & R_{+u,+u} \end{bmatrix}. \tag{5}$$

[Please insert Figure 1 here]

Then, the probabilities $R_{j,k}$ can be computed using the formula (Castagliola, Maravelakis, and Figueiredo 2016),

$$R_{j,k} = F_{\tilde{Y}}\left[\frac{H_k+\Delta-(1-\lambda)H_j}{\lambda}|n\right] - F_{\tilde{Y}}\left[\frac{H_k-\Delta-(1-\lambda)H_j}{\lambda}|n\right], \tag{6}$$

where $F_{\tilde{Y}}(\cdot\,|n)$ denotes the cumulative distribution function (c.d.f.) of the sample median $\tilde{Y}_i$, for $i \in \{1, 2, \ldots\}$, i.e. $F_{\tilde{Y}}(w|n) = F_\beta\left(\Phi\left(\frac{w-\mu_0}{\sigma_0} - \delta\right)|\frac{n+1}{2}, \frac{n+1}{2}\right)$. Here, $\Phi(\cdot)$ and $F_\beta(\cdot\,|a, b)$ represent the c.d.f.s of the standard normal distribution and beta distribution with parameters (a, b), respectively. Also, we define $\mathbf{p}_{\text{ini}} = (p_{-u}, \ldots, p_0, \ldots, p_u)^T$ as an initial probability vector with dimension $(2u + 1, 1)$ corresponding to the $2u + 1$ transient states, such that

$$p_j = \begin{cases} 1, \text{if } Z_0 \in (H_j - \Delta, H_j + \Delta] \\ 0, \text{if } Z_0 \notin (H_j - \Delta, H_j + \Delta] \end{cases}. \tag{7}$$

When the matrix **R** has a sufficiently large number of subintervals $2u + 1$ (for example, u = 200, $2u + 1 = 401$), this finite method gives an accurate evaluation of the RL characteristics of the Case-K EWMA $\tilde{X}$ chart. Note that we can consider the zero-state RL of the Case-K EWMA $\tilde{X}$ chart as a discrete phase-type random variable having parameters $(\mathbf{R}, \mathbf{p}_{\text{ini}})$ (refer to Neuts 1981; Latouche and Ramaswami 1999). Hence, the zero-state probability density function (p.d.f.) $f_{RL}(\ell)$ and c.d.f. $F_{RL}(\ell)$ of the RL distribution are equal to

$$f_{\text{RL}}(\ell) = Pr(\text{RL} = \ell) = \mathbf{p}_{\text{ini}}^T \mathbf{R}^{\ell-1} \mathbf{r} \tag{8}$$

and

$$F_{\text{RL}}(\ell) = Pr(\text{RL} \leq \ell) = 1 - \mathbf{p}_{\text{ini}}^T \mathbf{R}^{\ell} \mathbf{1}, \tag{9}$$

respectively, where $\ell \in \{1, 2, \ldots\}$. Then, the zero-state $(100\beta)^{\text{th}}$ percentile of the RL distribution, i.e. ℓ_β can be computed using (Gan, 1993)

$$Pr(\text{RL} \leq \ell_\beta - 1) \leq \beta \text{ and } Pr\left(\text{RL} \leq \ell_\beta\right) > \beta, \tag{10}$$

for $0 < \beta < 1$. Here, we can obtain the zero-state percentile of the Case-K RL distribution by using both Equations (9) and (10). Note that when $\beta = 0.5$, $\ell_{0.5}$ is the Case-K MRL value. The zero-state Case-K ARL and SDRL values can be computed as

$$\mathrm{ARL} = v_1 \tag{11}$$

and

$$\mathrm{SDRL} = \sqrt{\mathrm{E2RL} - \mathrm{ARL}^2}, \tag{12}$$

respectively. Here,

$$\mathrm{E2RL} = v_1 + v_2, \tag{13}$$

where v_1 and v_2 represent the 1st and 2nd factorial moments of the RL given as

$$v_1 = \mathbf{p}_{\mathrm{ini}}^T(\mathbf{I} - \mathbf{R})^{-1}\mathbf{1} \tag{14}$$

and

$$v_2 = 2\mathbf{p}_{\mathrm{ini}}^T(\mathbf{I} - \mathbf{R})^{-2}\mathbf{R}\mathbf{1}, \tag{15}$$

respectively, while $\mathbf{I}$ denotes the identity matrix of size $(2u + 1, 2u + 1)$.

The steady-state percentile of the RL distribution, ARL and SDRL of the Case-K EWMA $\tilde{X}$ chart can also be computed by applying the Markov chain method mentioned above, but by using the steady-state probability vector $\mathbf{p}_{\mathrm{ss}}$ instead of the initial probability vector $\mathbf{p}_{\mathrm{ini}}$. Due to the fact that the tpm $\mathbf{P}$ in Equation (4) is not ergodic, Lucas and Saccucci (1990) noted that the exact steady-state probability vector is not available. To make the tpm $\mathbf{P}$ ergodic, they suggested using the cyclical steady-state probability vector which can be obtained by modifying the tpm $\mathbf{P}$ such that the plotting statistic is reset back to state (0) when it is in the OOC state, i.e. (Lucas and Saccucci, 1990)

$$\mathbf{P}^* = \begin{pmatrix} \mathbf{R} & \mathbf{r} \\ 0 \ldots 1 \ldots 0 & 0 \end{pmatrix}. \tag{16}$$

Note that we can obtain $\mathbf{p}_{\text{ss}}$ by solving $\mathbf{p} = \mathbf{P}^{*T}\mathbf{p}$ such that $\mathbf{1}^T\mathbf{p} = 1$. Then, $\mathbf{p}_{\text{ss}} = (\mathbf{1}^T\mathbf{q})^{-1}\mathbf{q}$, where $\mathbf{q}$ represents a vector of length $2u + 1$ obtained from $\mathbf{p}$ by removing the entry associated with the absorbing state, such that the sum of all probabilities in $\mathbf{p}_{\text{ss}}$ is equal to 1. Hence, the cyclical steady-state $f_{RL}(\ell), F_{RL}(\ell)$, percentile of the RL distribution, ARL and SDRL can be computed in the same way as that for the zero-state case, but by replacing $\mathbf{p}_{\text{ini}}^T$ with $\mathbf{p}_{\text{ss}}^T$ in Equations (8) to (15).

3. The EWMA $\tilde{X}$ chart when parameters are unknown

In practical situations, the IC process mean and standard deviation, i.e. μ_0 and σ_0 are usually unknown and we have to estimate them from a Phase-I historical sample. Castagliola et al. (2016) showed that the estimators of μ_0 and σ_0 for the $\tilde{X}$-type chart are

$$\widehat{\mu_0} = \frac{1}{m}\sum_{i=1}^{m}\tilde{X}_i \tag{17}$$

and

$$\widehat{\sigma_0} = \frac{1}{d_{2,n}}\left(\frac{1}{m}\sum_{i=1}^{m}R_i\right), \tag{18}$$

respectively. Here, $\tilde{X}_i$ and $R_i = X_{i,(n)} - X_{i,(1)}$ denote the sample median and the range of subgroup i, respectively, and the constant $d_{2,n}$ can be obtained easily from any Statistical Quality Control text book. Then, the $\widehat{UCL}$ and $\widehat{LCL}$ of the Case-U EWMA $\tilde{X}$ chart can be easily obtained using Equations (3a) and (3b), respectively, by replacing K, μ_0 and σ_0 with K', $\hat{\mu}_0$ and $\hat{\sigma}_0$, where K' is a positive constant for Case-U.

For the Case-U EWMA $\tilde{X}$ chart, we may consider the standardized EWMA plotting statistic as an alternative to that in Equation (2). The standardized EWMA plotting statistic for the i^{th} sample is given as

$$Z_i' = (1-\lambda)Z_{i-1}' + \lambda\left(\frac{\tilde{Y}_i-\mu_0}{\sigma_0}\right), \tag{19}$$

where $Z_0' = 0$. Then, the corresponding modified $\widehat{UCL}'$ and $\widehat{LCL}'$ control limits of the Case-U EWMA $\tilde{X}$ chart are

$$\widehat{UCL}' = U + K'W \tag{20a}$$

and

$$\widehat{LCL}' = U - K'W, \tag{20b}$$

respectively, where $U = \frac{\hat{\mu}_0'-\mu_0}{\sigma_0}$ and $W = \frac{\hat{\sigma}_0'}{\sigma_0}$. The zero-state unconditional p.d.f. and c.d.f. i.e. $f_{RL}(\ell)$ and $F_{RL}(\ell)$ of the Case-U EWMA $\tilde{X}$ chart are (Castagliola et al., 2016)

$$f_{RL}(\ell) = \int_{-\infty}^{+\infty}\int_{0}^{+\infty}[f_U(u|m,n) \times f_V(v|m,n)]\hat{f}_{RL}(\ell)dwdu \tag{21}$$

and

$$F_{RL}(\ell) = 1 - \int_{-\infty}^{+\infty}\int_{0}^{+\infty}[f_U(u|m,n) \times f_V(v|m,n)]\hat{F}_{RL}(\ell)dwdu, \tag{22}$$

respectively, where $\hat{f}_{RL}(\ell)$ and $\hat{F}_{RL}(\ell)$ are the conditional p.d.f. and c.d.f. obtained through Equations (8) and (9), respectively, by replacing μ_0 and σ_0 with $\hat{\mu}_0'$ and $\hat{\sigma}_0'$.

Next, similar to Case-K, we can obtain the zero-state percentile of the Case-U RL distribution by using both Equations (22) and (10). Based on Equations (22) and (10) when $\beta = 0.5$, $\ell_{0.5}$ is the Case-U MRL value. The zero-state Case-U ARL and SDRL values can be computed as

$$\text{ARL} = \int_{-\infty}^{+\infty}\int_{0}^{+\infty}[f_U(u|m,n) \times f_V(v|m,n)]\hat{v}_1 dwdu \tag{23}$$

and

$$\text{SDRL} = \sqrt{\text{E2RL} - \text{ARL}^2}, \tag{24}$$

respectively, where

$$\text{E2RL} = \int_{-\infty}^{+\infty}\int_{0}^{+\infty}[f_U(u|m,n) \times f_V(v|m,n)](\hat{v}_1 + \hat{v}_2)dwdu. \tag{25}$$

Note that $\hat{v}_1$ and $\hat{v}_2$ can be obtained from Equations (14) and (15), respectively, by replacing μ_0 and σ_0 with $\hat{\mu}_0'$ and $\hat{\sigma}_0'$. There is no closed-form formulae for $f_U(u|m,n)$ and $f_V(v|m,n)$, hence Castagliola & Figueiredo (2013) provided a good approximation for them and the details are not repeated here due to space constraints. Also, it is worth mentioning that the cyclical steady-state Case-U $f_{RL}(\ell), F_{RL}(\ell)$, percentile of the RL distribution, ARL and SDRL can be computed in the same way as that for the zero-state case, but by replacing $\mathbf{p}_{\text{ini}}^T$ with $\mathbf{p}_{\text{ss}}^T$ in Equations (21) to (25).

4. Performance of the Case-K EWMA $\tilde{X}$ chart in terms of the ARL, SDRL, and percentiles of the RL distribution

We present the results of ARL, SDRL and percentiles of the RL distribution for the Case-K EWMA $\tilde{X}$ chart based on zero- and steady-state cases in Tables 1 and 2, respectively. The chart's optimal parameters (λ, K) of the Case-K EWMA $\tilde{X}$ chart were obtained through an optimization program written using the ScicosLab software. In these tables, we consider the desired IC ARL, $\text{ARL}_0 = 370$, sample sizes $n = \{3, 7\}$ and $\delta_{\text{opt}} = \{0.5, 2.0\}$. Here, δ_{opt} is the desired magnitude of a mean shift for which a fast detection is required. Note that the ARL, SDRL and percentiles of the RL distribution in these tables are computed for different shift sizes of $\delta = \{0, 0.1, 0.2, 0.4, 0.5, 0.6, 0.8, 1.0, 1.5, 2.0\}$, based on the chart's optimal parameters (λ, K).

[Please insert Tables 1 and 2 here]

From Tables 1 and 2, for both the zero- and steady-state cases, respectively, we observe that the ARL value is larger than the 50$^{\text{th}}$ percentile of the RL distribution, i.e. the MRL, except for some cases where mean shifts δ are large. Moreover, we notice that the difference between

ARL and MRL values reduces as the shift in the process mean increases. This shows that the skewness of the RL distribution changes according to the size of the mean shift, where the RL distribution is highly right-skewed when the process is IC or slightly OOC, and it becomes almost symmetric when the process is OOC. Therefore, special caution is needed in the interpretation of the RL distribution based only on the ARL. For instance, for the IC case of $ARL_0 = 370$ in Table 1, where $n = 3$ and $\delta_{\text{opt}} = 0.5$, practitioners may falsely conclude that a false alarm will be signalled by the 370th sample in half of the time. However, in reality, the ARL_0 is located between the 60th and 70th percentiles of the RL distribution, where a false alarm actually happens earlier, i.e. by the 257th sample, where the IC MRL $(MRL_0) = 257$, in half of the time. Moreover, still considering the same case in Table 1 but with $\delta = 2.0$, the ARL_1 is 2.77 and the OOC signal almost happens the same time, i.e. by the 3rd sample, where the OOC MRL $(MRL_1) = 3$, in half of the time. This particular example shows that for a highly right-skewed RL distribution, the median is always smaller than the average. However, for an almost symmetric RL distribution, the median is about the same as the average. Since the interpretation of the ARL for a symmetric RL distribution is certainly different from that of a highly right-skewed RL distribution, we recommend the use of the MRL as a more appropriate representation of the central tendency compared to the ARL.

The percentiles of the RL distribution are able to give more information related to the behaviour of a control chart. When $\delta = 0$, the lower percentiles, for instance, the 5th, 10th and 20th percentiles of the RL distribution, give some useful information about the early false alarms of the IC process. Using $n = 3$, $\delta_{\text{opt}} = 0.5$ and $\delta = 0$ in Table 2 as an example, there is a 10% probability for an early false alarm to take place by the 40th sample. This finding is interesting as it shows that although the ARL_0 value (=370) is relatively large, the values of the lower percentiles are relatively

small, indicating that a large number of false alarms happens when the process monitoring starts. Moreover, higher percentiles, for instance the 80th, 90th and 95th percentiles of the RL distribution give practitioners extra information regarding the process. For example, when n = 7, $\delta_{\text{opt}} = 0.5$ and $\delta = 1.0$ in Table 2, practitioners can claim with 95% confidence that an OOC will be signalled by the 6th sample.

Moreover, it is crucial for practitioners to pay attention on the spread of the RL distribution. The difference between the 95th and 5th percentiles of the RL distribution gives important clues about the skewness, spread and variation of the RL distribution. In Tables 1 and 2, we notice that as the value of δ increases, the difference between the 95th and 5th percentiles decreases. Taking the case of n = 7 and $\delta_{\text{opt}} = 0.5$ in Table 2 as an example, for $\delta = 0.2$, the difference between the 5th and 95th percentiles is 107; whereas for $\delta = 1.5$, the difference between the same percentiles is only 2. This indicates that for IC and slightly OOC processes, the spread of the RL distribution is large; whereas for a large OOC process, there is less variability in the RL distribution. Hence, interpretation using the ARL alone is inappropriate and misleading as the level of spread in the RL distribution of the EWMA $\tilde{X}$ chart varies according to the size of the mean shift. The ARL only gives the expected number of points that are needed to be plotted on a control chart prior to obtaining an OOC signal or a false alarm. It is not an indicator of the probability of getting an OOC signal or false alarm by a particular number of samples. Therefore, we need to propose an alternative performance measure for the EWMA $\tilde{X}$ chart. It is interesting to note that the MRL is a more reliable criterion as it is less influenced by the skewness of the RL distribution compared to the ARL. In addition, the MRL indicates that the EWMA $\tilde{X}$ chart will signal by a certain number of samples in 50% of the time or with 50% certainty.

5. Optimization designs of the EWMA $\tilde{X}$ chart based on MRL and EMRL

In this section, we discuss the optimization designs of the Case-K EWMA $\tilde{X}$ chart, that is, by minimizing the (i) MRL_1 and (ii) OOC EMRL ($EMRL_1$) for known and unknown mean shift sizes, respectively. When the mean shift size is known a priori, the optimization design of the Case-K EWMA $\tilde{X}$ chart based on the MRL is performed by minimizing the MRL_1, where the desired IC MRL (MRL_0) is predefined by the user. For the Case-K EWMA $\tilde{X}$ chart, λ and K are the two parameters that need to be optimized. In the following, we outline the detailed steps to determine the Case-K EWMA $\tilde{X}$ chart's optimal parameters (λ, K) when the mean shift size is known:

Step 1. Input the MRL_0, n, and δ_{opt} values.

Step 2. Initialize both the λ and K parameters with a small value such as 0.01.

Step 3. By using nonlinear equation solver, vary the parameters (λ, K) simultaneously so that the MRL_0 value in Step 1 is satisfied.

Step 4. Calculate the MRL_1 value using Equations (9) and (10), where $\beta = 0.5$, based on the current combination of parameters (λ, K) obtained in Step 3.

Step 5. Repeat Steps 3 to 4 and determine all the possible combinations of parameters (λ, K) together with their corresponding MRL_1 value.

Step 6. Choose the combination of parameters (λ, K) that results in the smallest MRL_1 value as the chart's optimal parameters.

The assumption that the mean shift size is known a priori, is too restrictive. In various situations, the magnitude of an exact mean shift size in a process is usually unknown. The above optimization design, based on minimizing MRL_1, may perform badly if the actual mean shift size deviates from the δ_{opt} value. For instance, consider the zero-state case of the Case-K EWMA $\tilde{X}$ chart with $n = 5$ and $\delta_{\text{opt}} = 0.8$ having optimal parameters $(\lambda, K) = (0.5001, 0.9227)$ and $MRL_1 = 5$ in Table 3.

If we use these parameters (λ, K) for the situation where the actual mean shift size is 0.2, the computed $\text{MRL}_1 = 83$, which results in an undesirable relative error of $100 \times (83 - 35)/35 = 137\%$ compared to the optimal $\text{MRL}_1 = 35$ (refer to Table 3 where $n = 5$ and $\delta_{\text{opt}} = 0.2$). To circumvent the problem that arises due to limited knowledge regarding the actual mean shift size, we suggest to use an alternative performance measure, i.e. the expected MRL (EMRL) which performs well for a range of mean shift sizes.

Therefore, for the case of an unknown mean shift size, the optimization design of the EWMA $\tilde{X}$ chart based on EMRL is conducted by minimizing the EMRL_1, where the IC EMRL (EMRL_0) is predefined by the user. Here, the EMRL is computed by

$$\text{EMRL} = \int_{\delta_{\min}}^{\delta_{\max}} f_{\delta}(\delta)\text{MRL}(\delta)d\delta. \tag{26}$$

Since it is difficult to know the actual distribution of $f_{\delta}(\delta)$, several researchers, such as Castagliola, Celano, and Psarakis (2011) and Ou et al. (2012) assumed that the shift in the process mean follows the uniform, $U[\delta_{\min}, \delta_{\max}]$ distribution. The integral in Equation (26) is evaluated numerically using the Gauss-Legendre quadrature method. In the following, we outline the detailed steps to determine the EWMA $\tilde{X}$ chart's optimal parameters (λ, K) when the mean shift size is unknown:

Step 1. Input the EMRL_0, n, $\delta_{\min}$ and $\delta_{\max}$ values.

Steps 2–6. Similar to Steps 2–6 when the mean shift size is known, but by replacing MRL_0 with EMRL_0 and MRL_1 with EMRL_1.

Note that the optimization designs of the Case-U EWMA $\tilde{X}$ chart can be obtained in the same way as that for the Case-K EWMA $\tilde{X}$ chart, but by replacing K of Case-K MRL and Case-K EMRL with K' of Case-U MRL and Case-U EMRL, followed by adding another input parameter m.

6. Performance studies

In this section, we compare the optimal Case-K EWMA $\tilde{X}$ and Case-K Shewhart $\tilde{X}$ charts, for both known and unknown mean shift sizes. Note that in these comprehensive comparative studies, we consider both the zero- and steady-state Case-K MRL and EMRL performances. Here, the *UCL* and *LCL* of the Case-K Shewhart $\tilde{X}$ chart are computed by using Equations (3a) and (3b), respectively, but by replacing the constant *K* with *L*, where $L > 0$ is the control limit coefficient of the Shewhart $\tilde{X}$ chart. Moreover, we evaluate the performances of the optimal EWMA $\tilde{X}$ chart under Case-U situations.

6.1 Performance comparisons between the Case-K EWMA $\tilde{X}$ and Shewhart $\tilde{X}$ charts when the shift size is known

We present the zero- and steady-state Case-K performances of the optimal EWMA $\tilde{X}$ and Shewhart $\tilde{X}$ charts for the desired IC MRL, $\text{MRL}_0 \in \{250, 370\}$ in Tables 3 and 4, respectively, where the shift size is known. Since the Shewhart $\tilde{X}$ chart is a memoryless-type control chart, its zero- and steady-state Case-K performances are exactly the same and we only present the zero-state results. In these tables, we consider the cases where $n \in \{3, 5, 7, 9, 11\}$ and $\delta_{\text{opt}} \in \{0.1, 0.2, 0.4, 0.6, 0.8, 1.0, 1.5, 2.0\}$. For each case, we present the optimal parameters (λ, *K*) and parameter *L* of the Case-K EWMA $\tilde{X}$ and Shewhart $\tilde{X}$ charts, respectively, and their corresponding 5$^{\text{th}}$ ($\ell_{0.05}$), 50$^{\text{th}}$ (MRL) and 95$^{\text{th}}$ ($\ell_{0.95}$) percentiles of the RL distribution. Note that the difference between the $\ell_{0.05}$ and $\ell_{0.95}$ can be used to determine the spread and variation of the RL distribution. Also, similar to Castagliola et al. (2016), we set $\lambda \geq 0.1$ for the convergence of the Markov chain approach.

[Please insert Tables 3–4 here]

From Tables 3 and 4, we observe that under both the zero- and steady-state cases, the optimal Case-K EWMA $\tilde{X}$ chart outperforms the Case-K Shewhart $\tilde{X}$ chart for small and moderate shifts in the process mean, since the EWMA $\tilde{X}$ chart gives a smaller MRL_1 value compared to the Shewhart $\tilde{X}$ chart. However, for large shifts in the process mean, the optimal Case-K EWMA $\tilde{X}$ chart has an almost similar performance to the Case-K Shewhart $\tilde{X}$ chart. Taking the case of $MRL_0 = 250$, $n = 3$ and $\delta_{\text{opt}} = 0.1$ (small shift) in Table 3 as an example, the zero- and steady-state MRL_1s of the EWMA $\tilde{X}$ chart are equal to 122 and 121, respectively; whereas the MRL_1 of the Shewhart $\tilde{X}$ chart is 227. Still considering this case but with $\delta_{\text{opt}} = 2.0$ (large shift), the zero- and steady-state MRL_1s of the Case-K EWMA $\tilde{X}$ and Case-K Shewhart $\tilde{X}$ charts are both equal to 2. This result is expected, as the EWMA procedure greatly outperforms the Shewhart procedure for small and moderate shifts in the process mean; whereas they have comparable performance for large shifts in the process mean.

Still investigating Tables 3 and 4, we also notice that the zero- and steady-state MRL_1s of the Case-K EWMA $\tilde{X}$ chart have comparable performances. For example, in Table 4, when $MRL_0 = 370$, $n = 3$ and $\delta_{\text{opt}} = 0.1$, the zero- and steady-state MRL_1s of the Case-K EWMA $\tilde{X}$ chart are equal to 164 and 162, respectively, and a similar trend is observed for other cases. In addition, it is interesting to note that the Case-K EWMA $\tilde{X}$ chart shows a smaller variation in the RL distribution compared to the Case-K Shewhart $\tilde{X}$ chart for small and moderate mean shift sizes, i.e. $0.1 \leq \delta_{\text{opt}} \leq 1.0$. This is shown by a smaller difference between the $\ell_{0.05}$ and $\ell_{0.95}$ values of the former compared to the latter. However, for large mean shift sizes, i.e. $\delta_{\text{opt}} \geq 1.5$, both the Case-K EWMA $\tilde{X}$ and Shewhart $\tilde{X}$ charts have comparable variation in the RL distribution. For example,

by considering the steady-state case of $\text{MRL}_0 = 370$, $n = 7$ and $\delta_{\text{opt}} = 0.2$ in Table 4, the variation in the RL distribution for the EWMA $\tilde{X}$ chart is $104 - 7 = 97$; whereas that for the Shewhart $\tilde{X}$ chart is $779 - 14 = 765$. However, when the shift size increases to $\delta_{\text{opt}} = 2.0$, the variation in the RL distribution for the EWMA $\tilde{X}$ chart is $2 - 1 = 1$, which is similar to that of the Shewhart $\tilde{X}$ chart.

6.2 Performance comparisons between the EWMA $\tilde{X}$ and Shewhart $\tilde{X}$ charts when the shift size is unknown

Table 5 presents the Case-K EWMA $\tilde{X}$ and Shewhart $\tilde{X}$ charts' optimal parameters (λ, K) and parameter L, respectively, and their corresponding minimized EMRL_1 value computed based on Equation (26), for a range of shift sizes from $\delta_{\min} = 0.1$ to $\delta_{\max} = 2.0$. Note that in this study, we consider the desired IC EMRL value, $\text{EMRL}_0 = 370$ and $n \in \{3, 5, 7, 9, 11\}$. Moreover, in Table 5, based on these computed optimal parameters (λ, K) and parameter L of the Case-K EWMA $\tilde{X}$ and Shewhart $\tilde{X}$ charts, respectively, we give the corresponding $(\ell_{0.05}, \text{MRL}_1, \ell_{0.95})$ values for $\delta \in \{0.1, 0.2, 0.4, 0.6, 0.8, 1.0, 1.5, 2.0\}$. For example, in Table 5, when $n = 5$ and $\delta = 0.1$, the values of $(\ell_{0.05}, \text{MRL}_1, \ell_{0.95})$ for the zero-state case of the Case-K EWMA $\tilde{X}$ chart are (18, 126, 509), corresponding to the optimal parameters (λ, K) = (0.1042, 0.3583) obtained based on minimizing EMRL_1.

[Please insert Table 5 here]

From Table 4, when $n = 7$ and $\delta = 0.2$, the steady-state chart's optimal parameters and MRL_1 value for the Case-K EWMA $\tilde{X}$ chart are (λ, K) = (0.1000, 0.2996) and $\text{MRL}_1 = 32$,

respectively; whereas for the same case, we obtain $\mathrm{MRL}_1 = 34$ based on the global chart's parameters (λ, K) = (0.1281, 0.3489) in Table 5. This example indicates that the MRL_1 value computed based on the global chart's parameters presented in Table 5 is close to the MRL_1 value for a specific mean shift size presented in Table 4. Therefore, the global charts' parameters of the Case-K EWMA $\tilde{X}$ and Shewhart $\tilde{X}$ charts presented in Table 5 are robust alternatives to the charts' parameters for a specific mean shift size given in Table 4, particularly when the exact shift size is unknown.

The results in Table 5 show that the optimal Case-K EWMA $\tilde{X}$ chart is superior to the Case-K Shewhart $\tilde{X}$ chart based on the EMRL_1 performance measure, for a range of shift sizes from $\delta_{\min} = 0.1$ to $\delta_{\max} = 2.0$. Moreover, in Table 5, the optimal Case-K EWMA $\tilde{X}$ chart has a better zero- and steady-state MRL_1 performances in detecting small and moderate mean shift sizes ($\delta < 1.0$) compared to the Case-K Shewhart $\tilde{X}$ chart; whereas for large shift sizes ($\delta > 1.0$), the Case-K Shewhart $\tilde{X}$ chart demonstrates a similar or slightly superior performance to the Case-K EWMA $\tilde{X}$ chart. In terms of the variation in the RL distribution, the Case-K EWMA $\tilde{X}$ chart greatly outperforms the Case-K Shewhart $\tilde{X}$ chart for small and moderate mean shift sizes. For instance, for both the zero- and steady-state cases where $n = 9$ and $\delta = 0.6$ (moderate shift size) in Table 5, the variations of the RL distribution which can be measured by the difference between $\ell_{0.05}$ and $\ell_{0.95}$ are 8 and 27, respectively, for the Case-K EWMA $\tilde{X}$ and Shewhart $\tilde{X}$ charts. This study also shows that the Case-K EWMA $\tilde{X}$ chart has an almost similar variation in the RL distribution for both the zero- and steady-state cases.

6.3 Performances of the optimal EWMA $\tilde{X}$ chart under Case-U situation

We present the zero-state Case-U performance of the optimal EWMA $\tilde{X}$ chart for the desired $\text{MRL}_0 = 370$ in Table 6, where the shift size is known. The main purpose of this section is not to show the superiority of the optimal Case-U EWMA $\tilde{X}$ chart to the Case-U Shewhart $\tilde{X}$ chart but to examine the effect of parameters estimation on the performance of the optimal EWMA $\tilde{X}$ chart. Since we have demonstrated that the zero- and steady-states Case-K performances of the optimal EWMA $\tilde{X}$ chart are almost the same in Section 6.1, we only present the zero-state Case-U results of the optimal EWMA $\tilde{X}$ chart in this subsection. Note that in Table 6, we display the chart's optimal parameters (λ, K) of the Case-U EWMA $\tilde{X}$ chart, followed by the corresponding $(\ell_{0.05}, \text{MRL}_1, \ell_{0.95})$ values for $n \in \{3, 5, 7, 9\}$, $m \in \{10, 20, 40, 80, 100000\}$ and $\delta \in \{0.1, 0.2, 0.4, 0.6, 0.8, 1.0, 1.5, 2.0\}$. Due to space constraint, we did not present the EMRL_1 results of the optimal Case-U EWMA $\tilde{X}$ chart when the shift size is unknown.

[Please insert Table 6 here]

In Table 6, the zero-state Case-U results of the EWMA $\tilde{X}$ chart when m is large, i.e. $m = 100000$ approach the zero-state Case-K results of the EWMA $\tilde{X}$ chart in Table 4. For instance, when $n = 3$ and $\delta = 0.2$, the $(\ell_{0.05}, \text{MRL}_1, \ell_{0.95})$ values of the zero-state Case-U EWMA $\tilde{X}$ chart for $m = 100000$ are (13, 60, 225) (see Table 6); whereas the $(\ell_{0.05}, \text{MRL}_1, \ell_{0.95})$ values of the Case-K EWMA $\tilde{X}$ chart are (13, 60, 224) (see Table 4). This is expected, as taking a large number of Phase-I samples allows the process parameters to be accurately estimated, i.e. Case-K. For the same reason, we observe that the MRL_1 value of the Case-U EWMA $\tilde{X}$ chart generally decreases as m increases, where n and δ are fixed. For example, when $n = 5$ and $\delta = 0.4$ in Table 6, the MRL_1

value of the Case-U EWMA $\tilde{X}$ chart is 23 for m = 10; whereas the MRL_1 value decreases to 16 as m increases to 80.

Moreover, we observe that the optimal parameters computed for the Case-U EWMA $\tilde{X}$ chart is important, as it allows this chart to have a closer IC performance to the nominal MRL, i.e. $MRL_1 = 370$. For example, in Table 6, when n = 3, m = 10 and δ = 0.4, the MRL_0 value of the Case-U EWMA $\tilde{X}$ chart is 370, corresponding to the optimal parameters (λ, K) = (0.1104, 0.5840). However, for the same combination of n, m and δ, the optimal parameters (λ, K) = (0.1260, 0.5030) (see the last column of Table 6) will give a smaller value of MRL_0= 86 (when process parameters are estimated) using our computer program. Hence, the use of optimal parameters computed for the Case-U EWMA $\tilde{X}$ chart will result in better IC performance, i.e. with less false alarms, when the process parameters are not known and need to be estimated.

7. Real data example

We illustrate the application of the optimal EWMA $\tilde{X}$ chart based on minimizing the $EMRL_1$ in monitoring the diameter of forged piston rings. Note that these piston rings data are available in Montgomery (2013). A piston ring is a ring that fits in between the cylinder and piston of a combustion engine. The diameter of a piston ring is crucial in preventing engine damage. This is because as the temperature increases, the piston ring will also expand and it may collide with the cylinder and lead to engine breakdown. Hence, the diameter of piston rings must follow the standards for compression ring gaps as outlined by the Society of Automotive Engineers (SAE).

Due to the importance of the diameter of piston rings, in this study, the EWMA $\tilde{X}$ chart is applied to monitor the inner diameter of forged automobile piston rings. The Phase I data with m = 25 samples have been collected and presented in Table 7. It consists of $i = 1, 2, ..., m$ subgroups,

each having $n = 5$ observations, $X_{i,1}, X_{i,2}, \ldots, X_{i,n}$. We assume that the IC mean μ_0 and IC standard deviation σ_0 are both known and can be correctly estimated from the Phase I data. Then, for this Phase I data, the estimators of μ_0 and σ_0 for the $\tilde{X}$-type chart are computed as (Castagliola et al. 2016)

$$\widehat{\mu_0} = \frac{1}{m}\sum_{i=1}^{m} \tilde{X}_i = \frac{1}{25}\sum_{i=1}^{25} \tilde{X}_i = 74.00176$$

and

$$\widehat{\sigma_0} = \frac{1}{d_{2,n}}\left(\frac{1}{m}\sum_{i=1}^{m} R_i\right) = \frac{1}{2.326}\left(\frac{1}{25}\sum_{i=1}^{25} R_i\right) = 0.0100,$$

using Equations (17) and (18), respectively. Moreover, the quality practitioners who are familiar with this process, know from past experience that although the exact shift size is unknown, it falls between $\delta_{\min} = 0.1$ and $\delta_{\max} = 2.0$ and the process has gone into the steady-state.

Then, by assuming that $\text{EMRL}_0 = 370$, we obtain the EWMA $\tilde{X}$ chart's optimal parameters as (λ, K) = (0.1042, 0.3592) from Table 5. Using these chart's optimal parameters, we compute the *UCL* and *LCL* of the EWMA $\tilde{X}$ chart using Equations (3a) and (3b) as follows:

$$UCL = 74.00176 + (0.3592 \times 0.0100) = 74.0054$$

and

$$LCL = 74.00176 - (0.3592 \times 0.0100) = 73.9982,$$

respectively. After establishing the EWMA $\tilde{X}$ chart in Phase I, we proceed with Phase II monitoring of the piston rings process by taking 15 additional samples (see Table 8). For these samples, we compute the sample median values $\tilde{Y}_i$ and the EWMA sequence Z_i as presented in Table 8. Note that in Table 8, the boldfaced entries denote the OOC cases. Then, we plot the 15 Phase II samples, sample median values $\tilde{Y}_i$ and the EWMA sequence Z_i in Figures 2(a), 2(b) and 2(c), respectively. We observe in Figure 2(c) that the optimal EWMA $\tilde{X}$ chart detects the first OOC

signal at sample 10, since this is the first sample that falls beyond the UCL. Note that the optimal EWMA $\tilde{X}$ chart also declares other OOC signals at samples 12, 13, 14 and 15. Since the OOC signals are declared by the EWMA $\tilde{X}$ chart, a quick corrective action should be taken to identify and remove the assignable cause(s), and bring the process back into the IC situation.

[Please insert Tables 7–8 here]

[Please insert Figure 2 here]

8. Conclusions

An in-depth understanding of a control chart's performance characteristics is crucial as it increases practitioners' confidence in applying it. In the existing EWMA-type charts, the use of ARL alone to represent the skewed RL distribution has caused some vital information on the RL distribution to be neglected. This article demonstrates that the percentiles of the RL distribution are better performance measures compared to the ARL. Among all the percentiles of the RL distribution, we focus on the 5^{th}, 50^{th} (i.e. MRL) and 95^{th} percentiles of the RL distribution. This is because the MRL is a better measure of central tendency compared to the ARL when the RL distribution is skewed, and the difference between the 5^{th} and 95^{th} percentiles gives information regarding the spread and variation of the RL distribution.

Therefore, in this article, we develop an optimal EWMA $\tilde{X}$ chart based on minimizing the MRL_1 and $EMRL_1$, for known and unknown mean shift sizes, respectively. Note that the optimization design based on minimizing the EMRL provides us with the chart's optimal parameters which performs favourably for a range of shift sizes, i.e. from $\delta_{\min}$ to $\delta_{\max}$ when the exact shift size is not known in advance. These chart's optimal parameters presented in Tables 3

to 5 are useful to quality practitioners as these tables facilitate a quick implementation of the EWMA $\tilde{X}$ chart. From the performance comparison, we observe that the EWMA $\tilde{X}$ chart consistently outperforms the Shewhart $\tilde{X}$ chart for small and moderate shift sizes; whereas both charts have a comparable performance for large shift sizes. Moreover, when the exact shift size is unknown, the EWMA $\tilde{X}$ chart is superior to the Shewhart $\tilde{X}$ chart in terms of the EMRL performance. In addition, we study the effect of parameters estimation on the performance of the optimal EWMA $\tilde{X}$ chart. We present a real life example to demonstrate the application of the EWMA $\tilde{X}$ chart based on EMRL. In conclusion, the proposed optimization designs of the EWMA $\tilde{X}$ chart based on MRL and EMRL are useful alternative design criteria for practitioners in the design and implementation of this control chart.

Acknowledgement

This research is supported by the Universiti Tunku Abdul Rahman (UTAR), Fundamental Research Grant Scheme (FRGS), no. FRGS/1/2019/STG06/UTAR/02/2.

References

Abbas, N., M. Riaz, and R. J. M. M. Does. 2013. CS-EWMA chart for monitoring process dispersion. *Quality and Reliability Engineering International* 29 (5): 653–663.

Bischak, D. P., and D. Trietsch. 2007. The rate of false signals in Ū control charts with estimated limits. *Journal of Quality Technology* 39 (1): 54–65.

Brook, D., and D. Evans. 1972. An approach to the probability distribution of CUSUM run length. *Biometrika* 59 (3): 539–549.

Castagliola, P. 2001. An-EWMA control chart for monitoring the process sample median. *International Journal of Reliability, Quality and Safety Engineering* 8 (2): 123–135.

Castagliola, P., G. Celano, and S. Psarakis. 2011. Monitoring the coefficient of variation using EWMA charts. *Journal of Quality Technology* 43 (3): 249–265.

Castagliola, P., P. E. Maravelakis, and F. O. Figueiredo. 2016. The EWMA median chart with estimated parameters. *IIE Transactions* 48 (1): 66–74.

Chakraborti, S. 2007. Run length distribution and percentiles: the Shewhart $\bar{X}$ chart with unknown parameters. *Quality Engineering* 19 (2): 119–127.

Chong, Z. L., M. B. C. Khoo, W. L. Teoh, H. W. You, and P. Castagliola (2019b). Optimal design of side sensitive modified group runs (SSMGR) chart when process parameters are estimated. *Quality and Reliability Engineering International* 35 (1): 246–262.

Chong, Z. L., M. B. C. Khoo, W. L. Teoh, W. C. Yeong, and S. L. Lim (2020). Optimal design of the modified group runs (MGR) $\bar{X}$ chart when process parameters are estimated. *Communications in Statistics - Simulation and Computation* 49 (1): 244–260.

Eleftheriou, M., and N. Farmakis. 2016. A continuous sampling plan based on EWMA control chart rules. *Quality Technology & Quantitative Management* 13 (1): 16–28.

Gan, F. F. 1993. An optimal design of EWMA control charts based on median run length. *Journal of Statistical Computation and Simulation* 45 (3–4): 169–184.

Hu, X. L., P. Castagliola, X. J. Zhou, and A. A. Tang. 2019. Conditional design of the EWMA median chart with estimated parameters. *Communications in Statistics – Theory and Methods* 48 (8): 1871–1889.

Human, S. W., P. Kritzinger, and S. Chakraborti. 2011. Robustness of the EWMA control chart for individual observations. *Journal of Applied Statistics* 38 (10): 2071–2087.

Janacek, G. J., and S. E. Meikle. 1997. Control charts based on medians. *Journal of the Royal Statistical Society: Series D (The Statistician)* 46 (1): 19–31.

Jensen, W. A., L. A. Jones–Farmer, C. W. Champ, and W. H. Woodall. 2006. Effects of parameters estimation on control chart properties: a literature review. *Journal of Quality Technology* 38 (4): 349–364.

Jones, L. A., C. W. Champ, and S. E. Rigdon. 2001. The performance of exponentially weighted moving average charts with estimated parameters. *Technometrics* 43 (2): 156–167.

Jones, L. A., C. W. Champ, and S. E. Rigdon. 2004. The run length distribution of the CUSUM with estimated parameters. *Journal of Quality Technology* 36 (1): 95–108.

Khoo, M. B. C. 2005. A control chart based on sample median for the detection of a permanent shift in the process mean. *Quality Engineering* 17 (2): 243–257.

Khoo, M. B. C., E. K. Tan, Z. L. Chong, and S. Haridy. 2015. Side-sensitive group runs double sampling (SSGRDS) chart for detecting mean shifts. *International Journal of Production Research* 53 (15): 4735–4753.

Khoo, M. B. C., V. H. Wong, Z. Wu, and P. Castagliola. 2011. Optimal designs of the multivariate synthetic chart for monitoring the process mean vector based on median run length. *Quality and Reliability Engineering International* 27 (8): 981–997.

Khoo, M. B. C., V. H. Wong, Z. Wu, and P. Castagliola. 2012. Optimal design of the synthetic chart for the process mean based on median run length. *IIE Transactions* 44 (9): 765–779.

Latouche, G., and V. Ramaswami. 1999. *Introduction to matrix analytic methods in stochastic modelling*. Philadelphia, PA: ASA SIAM.

Lee, M. H., and M. B. C. Khoo. 2017. Optimal designs of multivariate synthetic |S| control chart based on median run length. *Communications in Statistics–Theory and Methods* 46 (6): 3034–3053.

Lim, S. L., Yeong, W. C., Khoo, M. B. C., Chong, Z. L., and Khaw, K. W. 2019. An alternative design for the variable sample size coefficient of variation chart based on the median run length and expected median run length. *International Journal of Industrial Engineering*. In press.

Low, C. K., M. B. C. Khoo, W. L. Teoh, and Z. Wu. 2012. The revised *m*-of-*k* runs rule based on median run length. *Communications in Statistics–Simulation and Computation* 41 (8): 1463–1477.

Lucas, J. M., and M. S. Saccucci. 1990. Exponentially weighted moving average control schemes: Properties and enhancements. *Technometrics* 32 (1): 1–12.

Maravelakis, P.E., J. Panaretos, and S. Psarakis. 2005. An examination of the robustness to non-normality of the EWMA control charts for the dispersion. *Communications in Statistics–Simulation and Computation* 34 (4): 1069–1079.

Montgomery, D. C. 2013. *Statistical quality control: A modern introduction*. (7th edn). New York: John Wiley & Sons.

Neuts, M. F. 1981. *Matrix-geometric solutions in stochastic models: An algorithmic approach.* Baltimore: The Johns Hopkins University Press.

Ou, Y., Z. Wu, K. M. Lee, and S. Chen. 2012. An optimal design algorithm of the SPRT chart for minimizing weighted ATS. *International Journal of Production Economics* 139 (2): 564–574.

Page, E. S. 1954. Continuous inspection schemes. *Biometrika* 41 (1–2): 100–115.

Psarakis S, A. K. Vyniou, and P. Castagliola. 2014. Some recent developments on the effects of parameter estimation on control charts. *Quality and Reliability Engineering International* 30 (8): 1113–1129.

Roberts, S. W. 1959. Control chart tests based on geometric moving averages. *Technometrics* 1 (3): 239–250.

Shamsuzzaman, M., M. B. C. Khoo, S. Haridy, and I. Alsyouf. 2016. An optimization design of the combined Shewhart-EWMA control chart. *The International Journal of Advanced Manufacturing Technology* 86 (5–8): 1627–1637.

Sheu, S. H., and L. Yang. 2006. The generally weighted moving average control chart for monitoring the process median. *Quality Engineering* 18 (3): 333–344.

Simoes, B. F. T., E. K. Epprecht, and A. F. B. Costa. 2010. Performance comparisons of EWMA control chart schemes. *Quality Technology & Quantitative Management* 7 (3): 249–261.

Tang, A. A., P. Castagliola, J. Sun, and X. Hu. 2019a. Optimal design of the adaptive EWMA chart for the mean based on median run length and expected median run length. *Quality Technology & Quantitative Management* 16 (4): 439–458.

Tang, A. A., P. Castagliola, J. Sun, and X. Hu. 2019b. The adaptive EWMA median chart for known and estimated parameters. *Journal of Statistical Computation and Simulation* 89 (5): 844–863.

Teh, S. Y., M. B. C. Khoo, K. S. Ong, K. L. Soh, and W. L. Teoh. 2015. A study on the S2-EWMA chart for monitoring the process variance based on the MRL performance. *Sains Malaysiana* 44 (7): 1067-1075.

Teoh, W. L., J. K. Chong, M. B. C. Khoo, P. Castagliola, and W. C. Yeong. 2017. Optimal designs of the variable sample size chart based on median run length and expected median run length. *Quality and Reliability Engineering International* 33 (1): 121–134.

Teoh, W. L., M. B. C. Khoo, P. Castagliola, and S. Chakraborti. 2014. Optimal design of the double sampling $\bar{X}$ chart with estimated parameters based on median run length. *Computers & Industrial Engineering* 67, 104–115.

Yang, L., S. Pai, and Y. R. Wang. 2010. A novel CUSUM median control chart. *Proceedings of International Multiconference of Engineers and Computer Scientists* 3, 1707–1710.

Zwetsloot, I. M., and W. H. Woodall. 2017. A head-to-head comparative study of the conditional performance of control charts based on estimated parameters. *Quality Engineering* 29 (2): 244–253.

Zwetsloot, I. M., M. Schoonhoven, and R. J. M. M. Does. 2016. Robust point location estimators for the EWMA control chart. *Quality Technology & Quantitative Management* 13 (1): 29–38.

Table 1. Exact ARLs, SDRLs and percentiles of the RL distribution for the Case-K EWMA $\tilde{X}$ chart with the chart's optimal parameters (λ, K) corresponding to $n \in \{3, 7\}$, $\delta_{\text{opt}} \in \{0.5, 2.0\}$ and $\text{ARL}_0 = 370$, under the zero-state case.

			Percentiles of the RL distribution										
δ	ARL	SDRL	5th	10th	20th	30th	40th	50th	60th	70th	80th	90th	95th
$n = 3, \delta_{\text{opt}} = 0.5, (\lambda, K) = (0.1000, 0.4160)$													
0.0	370.00	368.50	26	46	88	136	191	257	337	440	586	835	1084
0.1	176.09	174.58	17	27	47	69	94	125	162	209	276	391	506
0.2	67.59	66.08	11	15	23	31	40	50	63	80	103	143	183
0.4	21.16	19.55	7	8	10	13	15	18	21	24	30	39	48
0.5	14.87	8.29	5	7	8	10	11	13	15	17	20	26	31
0.6	11.40	9.87	5	6	7	8	9	10	11	13	15	19	22
0.8	7.12	6.03	4	4	5	6	6	7	8	9	10	12	14
1.0	5.84	4.07	3	4	4	5	5	5	6	7	7	9	10
1.5	3.71	1.01	2	3	3	3	3	4	4	4	4	5	5
2.0	2.77	0.79	2	2	2	2	3	3	3	3	3	4	4
$n = 3, \delta_{\text{opt}} = 2.0, (\lambda, K) = (0.6856, 1.4550)$													
0.0	370.00	368.50	20	40	83	133	189	257	339	445	595	850	1106
0.1	308.95	307.44	17	33	70	111	158	214	283	372	496	710	923
0.2	201.86	200.36	11	22	46	73	104	140	185	243	324	463	602
0.4	74.13	72.62	5	9	18	27	39	52	68	89	119	169	219
0.5	46.44	44.92	4	6	11	17	24	33	43	56	74	105	136
0.6	29.98	28.44	3	4	8	12	16	21	28	36	47	67	87
0.8	14.37	12.79	2	3	4	6	8	10	13	17	22	31	40
1.0	8.04	6.37	2	2	3	4	5	6	8	9	12	17	21
1.5	3.08	0.49	1	1	2	2	2	3	3	4	4	6	7
2.0	1.81	1.47	1	1	1	1	1	2	2	2	2	3	3
$n = 7, \delta_{\text{opt}} = 0.5, (\lambda, K) = (0.1593, 0.3804)$													
0.0	370.00	368.50	24	44	86	135	190	257	338	442	589	840	1092
0.1	132.19	13068	13	20	35	51	71	93	121	157	208	295	382
0.2	42.17	40.64	7	10	15	19	25	31	39	50	64	89	113
0.4	12.01	10.40	4	5	6	8	9	10	12	14	17	21	26
0.5	8.43	6.76	3	4	5	6	7	7	8	10	11	14	17
0.6	6.47	4.74	3	3	4	5	5	6	7	7	8	10	12
0.8	4.44	2.52	2	3	3	3	4	4	5	5	6	7	7
1.0	3.41	1.18	2	2	3	3	3	3	4	4	4	5	5
1.5	2.26	1.29	2	2	2	2	2	2	2	2	3	3	3
2.0	1.82	1.47	1	1	2	2	2	2	2	2	2	2	2
$n = 7, \delta_{\text{opt}} = 2.0, (\lambda, K) = (0.9363, 1.2996)$													
0.0	370.00	368..50	19	39	83	132	189	257	339	445	595	851	1107
0.1	293.72	292.21	16	31	66	105	150	204	269	354	472	676	879
0.2	174.61	173.11	10	19	39	63	89	121	160	210	281	401	522
0.4	54.64	53.12	3	6	13	20	28	38	50	66	88	125	162
0.5	32.09	31.44	2	4	8	12	17	22	29	39	51	73	95
0.6	19.73	18.17	2	3	5	7	10	14	18	24	31	45	58
0.8	8.56	6.90	1	2	2	3	5	6	8	10	13	19	24
1.0	4.43	2.52	1	1	2	2	3	3	4	5	7	9	12
1.5	1.62	1.50	1	1	1	1	1	1	2	2	2	3	3
2.0	1.10	1.44	1	1	1	1	1	1	1	1	1	1	2

Table 2. Exact ARLs, SDRLs and percentiles of the RL distribution for the Case-K EWMA $\bar{X}$ chart with the chart's optimal parameters (λ, K) corresponding to $n \in \{3, 7\}$, $\delta_{\text{opt}} \in \{0.5, 2.0\}$ and $\text{ARL}_0 = 370$, under the steady-state case.

			Percentiles of the RL distribution										
δ	ARL	SDRL	5th	10th	20th	30th	40th	50th	60th	70th	80th	90th	95th
$n = 3, \delta_{\text{opt}} = 0.5, (\lambda, K) = (0.1000, 0.4166)$													
0.0	370.00	369.40	20	40	83	132	189	257	339	445	595	851	1107
0.1	174.99	169.28	14	24	44	66	92	123	161	210	278	395	513
0.2	66.70	58.87	9	13	21	29	39	49	62	79	103	143	184
0.4	20.71	14.00	5	7	10	12	15	17	20	24	30	39	48
0.5	14.59	8.74	4	6	8	9	11	13	15	17	20	26	31
0.6	11.42	9.81	5	6	7	8	9	10	11	13	15	19	22
0.8	7.23	6.05	4	4	5	6	6	7	8	9	10	12	14
1.0	5.76	2.44	2	3	4	4	5	5	6	7	8	9	10
1.5	3.68	1.35	2	2	3	3	3	4	4	4	5	5	6
2.0	2.76	0.94	1	2	2	2	2	3	3	3	4	4	4
$n = 3, \delta_{\text{opt}} = 2.0, (\lambda, K) = (0.6774, 1.4450)$													
0.0	370.00	369.50	19	39	83	132	189	257	339	445	595	851	1107
0.1	308.28	307.65	16	33	69	110	158	214	283	371	496	709	922
0.2	200.60	199.73	11	22	45	72	103	139	184	241	322	461	599
0.4	73.20	72.01	5	9	17	27	38	51	67	88	117	167	217
0.5	45.77	44.50	4	6	11	17	24	32	42	55	73	104	135
0.6	29.89	28.35	3	4	8	12	16	21	28	36	47	67	87
0.8	14.30	12.71	2	3	4	6	8	10	13	17	22	31	40
1.0	7.91	6.60	1	2	3	4	5	6	7	9	12	16	21
1.5	3.04	1.93	1	1	2	2	2	3	3	4	4	6	7
2.0	1.81	0.89	1	1	1	1	1	2	2	2	2	3	3
$n = 7, \delta_{\text{opt}} = 0.5, (\lambda, K) = (0.1592, 0.3807)$													
0.0	370.00	369.45	19	39	83	132	189	257	339	445	595	851	1107
0.1	131.55	126.98	11	18	33	50	70	93	121	158	209	297	385
0.2	41.67	36.1	6	9	14	19	24	31	39	49	64	89	113
0.4	11.78	7.42	3	4	6	7	9	10	12	14	17	21	26
0.5	8.27	4.54	3	3	5	6	6	7	8	10	11	14	17
0.6	6.48	4.75	3	3	4	5	5	6	7	7	8	10	12
0.8	4.44	2.53	2	3	3	3	4	4	5	5	6	7	7
1.0	3.37	1.29	2	2	2	3	3	3	4	4	4	5	6
1.5	2.23	0.75	1	1	2	2	2	2	2	3	3	3	3
2.0	1.74	0.56	1	1	1	1	2	2	2	2	2	2	3
$n = 7, \delta_{\text{opt}} = 2.0, (\lambda, K) = (0.9686, 1.2729)$													
0.0	370.00	369.50	19	39	83	132	189	257	339	445	595	851	1107
0.1	295.65	295.13	16	32	66	106	151	205	271	356	476	680	885
0.2	177.76	177.20	10	19	40	64	91	123	163	214	286	409	531
0.4	56.48	55.88	3	6	13	21	29	39	52	68	91	129	168
0.5	33.30	32.68	2	4	8	12	17	23	31	40	53	76	99
0.6	15.61	14.03	1	2	4	6	8	11	14	19	25	35	46
0.8	7.15	5.45	1	1	2	3	4	5	7	8	11	16	20
1.0	4.56	3.93	1	1	2	2	3	3	4	5	7	10	12
1.5	1.63	0.97	1	1	1	1	1	1	2	2	2	3	4
2.0	1.10	0.32	1	1	1	1	1	1	1	1	1	1	2

Table 3. Comparisons of the $(\ell_{0.05}, \mathrm{MRL}_1, \ell_{0.95})$ values for the Case-K Shewhart $\tilde{X}$ and optimal Case-K EWMA $\tilde{X}$ charts, together with the charts' corresponding parameters when $n \in \{3, 5, 7, 9, 11\}, \delta_{\mathrm{opt}} \in \{0.1, 0.2, 0.4, 0.6, 0.8, 1.0, 1.5, 2.0\}$ and $\mathrm{MRL}_0 = 250$.

		Shewhart $\tilde{X}$	EWMA $\tilde{X}$ (Zero state)	EWMA $\tilde{X}$ (Steady state)
n	δ_{opt}	L $(\ell_{0.05}, \mathrm{MRL}_1, \ell_{0.95})$	$(\lambda, K)(\ell_{0.05}, \mathrm{MRL}_1, \ell_{0.95})$	$(\lambda, K)(\ell_{0.05}, \mathrm{MRL}_1, \ell_{0.95})$
3	0.1	2.0210 (17, 227, 978)	(0.1001, 0.4143) (17, 122, 497)	(0.1000, 0.4152) (13, 121, 503)
	0.2	2.0210 (13, 175, 755)	(0.1001, 0.4143) (11, 50, 181)	(0.1000, 0.4152) (9, 49, 181)
	0.4	2.0210 (7, 85, 366)	(0.1625, 0.5603) (6, 18, 58)	(0.1250, 0.4775) (5, 17, 52)
	0.6	2.0210 (3, 40, 173)	(0.2501, 0.7334) (3, 10, 30)	(0.2500, 0.7329) (3, 10, 30)
	0.8	2.0210 (2, 20, 86)	(0.2501, 0.7334) (3, 6, 16)	(0.2500, 0.7329) (3, 6, 16)
	1.0	2.0210 (1, 11, 46)	(0.5000, 1.1543) (2, 5, 15)	(0.5000, 1.1548) (2, 5, 14)
	1.5	2.0210 (1, 3, 13)	(0.5000, 1.1543) (1, 3, 6)	(0.5000, 1.1548) (1, 2, 6)
	2.0	2.0210 (1, 2, 5)	(0.5000, 1.1543) (1, 2, 3)	(0.5000, 1.1548) (1, 2, 3)
5	0.1	1.6150 (16, 215, 928)	(0.1001, 0.3312) (15, 95, 378)	(0.1001, 0.3322) (12, 94, 382)
	0.2	1.6150 (11, 148, 638)	(0.1001, 0.3312) (9, 35, 119)	(0.1001, 0.3322) (7, 35, 120)
	0.4	1.6150 (5, 58, 250)	(0.1250, 0.3805) (5, 13, 33)	(0.1250, 0.3817) (4, 13, 33)
	0.6	1.6150 (2, 24, 102)	(0.2501, 0.5863) (3, 7, 18)	(0.2500, 0.5859) (3, 7, 18)
	0.8	1.6150 (1, 11, 46)	(0.5001, 0.9227) (2, 5, 14)	(0.5000, 0.9225) (2, 5, 14)
	1.0	1.6150 (1, 6, 23)	(0.5000, 0.9226) (1, 3, 8)	(0.5000, 0.9230) (1, 3, 8)
	1.5	1.6150 (1, 2, 6)	(0.5000, 0.9226) (1, 2, 4)	(0.5000, 0.9230) (1, 2, 4)
	2.0	1.6150 (1, 1, 3)	(0.5000, 0.9226) (1, 1, 2)	(0.5000, 0.9230) (1, 1, 2)
7	0.1	1.3818 (16, 204, 880)	(0.1001, 0.2837) (14, 78, 303)	(0.1021, 0.2880) (11, 77, 308)
	0.2	1.3818 (10, 127, 547)	(0.1001, 0.2837) (8, 28, 88)	(0.1157, 0.3114) (6, 28, 94)
	0.4	1.3818 (4, 42, 182)	(0.1250, 0.3259) (4, 10, 24)	(0.2500, 0.5026) (3, 10, 32)
	0.6	1.3818 (2, 16, 67)	(0.5001, 0.7898) (2, 6, 20)	(0.5000, 0.7896) (2, 6, 20)
	0.8	1.3818 (1, 7, 28)	(0.5001, 0.7898) (2, 4, 10)	(0.5000, 0.7896) (2, 4, 10)
	1.0	1.3818 (1, 4, 14)	(0.5000, 0.7897) (1, 3, 6)	(0.5000, 0.7901) (1, 3, 6)
	1.5	1.3818 (1, 1, 4)	(0.7500, 1.0683) (1, 1, 3)	(0.7501, 1.0685) (1, 1, 3)
	2.0	1.3818 (1, 1, 2)	(0.7500, 1.0683) (1, 1, 2)	(0.7600, 1.0800) (1, 1, 2)
9	0.1	1.2264 (15, 194, 836)	(0.1001, 0.2520) (13, 66, 252)	(0.1001, 0.2527) (10, 65, 254)
	0.2	1.2264 (9, 110, 476)	(0.1001, 0.2520) (8, 23, 70)	(0.1001, 0.2527) (6, 23, 70)
	0.4	1.2264 (3, 32, 139)	(0.2500, 0.4458) (3, 9, 24)	(0.1875, 0.3732) (3, 8, 22)
	0.6	1.2264 (1, 11, 47)	(0.5001, 0.7013) (2, 5, 15)	(0.5000, 0.7011) (2, 5, 15)
	0.8	1.2264 (1, 5, 19)	(0.5001, 0.7013) (1, 3, 7)	(0.5000, 0.7011) (1, 3, 7)
	1.0	1.2264 (1, 3, 9)	(0.5000, 0.7012) (1, 2, 5)	(0.5000, 0.7015) (1, 2, 5)
	1.5	1.2264 (1, 1, 3)	(0.5000, 0.7012) (1, 1, 2)	(0.5000, 0.7015) (1, 1, 2)
	2.0	1.2264 (1, 1, 1)	(0.5000, 0.7012) (1, 1, 2)	(0.5000, 0.7015) (1, 1, 2)
11	0.1	1.1137 (14, 185, 796)	(0.1001, 0.2290) (12, 57, 215)	(0.1001, 0.2297) (9, 57, 216)
	0.2	1.1137 (8, 97, 418)	(0.1001, 0.2290) (7, 20, 58)	(0.1001, 0.2297) (5, 20, 58)
	0.4	1.1137 (2, 26, 110)	(0.2500, 0.4050) (3, 7, 20)	(0.2500, 0.4056) (2, 7, 20)
	0.6	1.1137 (1, 9, 35)	(0.5001, 0.6370) (2, 4, 12)	(0.5000, 0.6368) (2, 4, 12)
	0.8	1.1137 (1, 4, 14)	(0.5001, 0.6370) (1, 3, 6)	(0.5000, 0.6368) (1, 3, 6)
	1.0	1.1137 (1, 2, 7)	(0.5000, 0.6369) (1, 2, 4)	(0.5000, 0.6372) (1, 2, 4)
	1.5	1.1137 (1, 1, 2)	(0.5000, 0.6369) (1, 1, 2)	(0.5000, 0.6372) (1, 1, 2)
	2.0	1.1137 (1, 1, 1)	(0.5000, 0.6369) (1, 1, 2)	(0.5000, 0.6372) (1, 1, 1)

Table 4. Comparisons of the $(\ell_{0.05}, \mathrm{MRL}_1, \ell_{0.95})$ values for the Case-K Shewhart $\tilde{X}$ and optimal Case-K EWMA $\tilde{X}$ charts, together with the charts' corresponding parameters when $n \in \{3, 5, 7, 9, 11\}, \delta_{\mathrm{opt}} \in \{0.1, 0.2, 0.4, 0.6, 0.8, 1.0, 1.5, 2.0\}$ and $\mathrm{MRL}_0 = 370$.

		Shewhart $\tilde{X}$	EWMA $\tilde{X}$ (Zero-state)	EWMA $\tilde{X}$ (Steady-state)
n	δ_{opt}	L $(\ell_{0.05}, \mathrm{MRL}_1, \ell_{0.95})$	(λ, K) $(\ell_{0.05}, \mathrm{MRL}_1, \ell_{0.95})$	(λ, K) $(\ell_{0.05}, \mathrm{MRL}_1, \ell_{0.95})$
3	0.1	2.1022 (25, 333, 1438)	(0.1000, 0.4370) (21, 164, 673)	(0.1000, 0.4376) (17, 162, 679)
	0.2	2.1022 (19, 253, 1092)	(0.1000, 0.4370) (13, 60, 224)	(0.1039, 0.4479) (10, 60, 230)
	0.4	2.1022 (9, 119, 512)	(0.0938, 0.4200) (7, 19, 53)	(0.0938, 0.4212) (6, 19, 53)
	0.6	2.1022 (5, 55, 234)	(0.2501, 0.7669) (4, 11, 35)	(0.2500, 0.7663) (4, 11, 35)
	0.8	2.1022 (2, 27, 114)	(0.2501, 0.7669) (3, 7, 18)	(0.2500, 0.7663) (3, 7, 18)
	1.0	2.1022 (2, 14, 59)	(0.5000, 1.2023) (2, 5, 17)	(0.5100, 1.2191) (2, 5, 17)
	1.5	2.1022 (1, 4, 15)	(0.5000, 1.2023) (1, 3, 6)	(0.5000, 1.2026) (1, 3, 6)
	2.0	2.1022 (1, 2, 6)	(0.5000, 1.2023) (1, 2, 3)	(0.5000, 1.2026) (1, 2, 3)
5	0.1	1.6799 (24, 315, 1359)	(0.1000, 0.3494) (18, 124, 499)	(0.1000, 0.3499) (15, 122, 503)
	0.2	1.6799 (16, 212, 915)	(0.1000, 0.3494) (11, 42, 144)	(0.1156, 0.3823) (8, 43, 156)
	0.4	1.6799 (6, 80, 344)	(0.1250, 0.4005) (6, 14, 37)	(0.1250, 0.4013) (4, 14, 37)
	0.6	1.6799 (3, 32, 135)	(0.2501, 0.6131) (3, 8, 20)	(0.2500, 0.6126) (3, 8, 20)
	0.8	1.6799 (1, 14, 59)	(0.5001, 0.9610) (2, 5, 17)	(0.5000, 0.9608) (2, 5, 16)
	1.0	1.6799 (1, 7, 28)	(0.5000, 0.9609) (2, 4, 9)	(0.5000, 0.9612) (1, 4, 9)
	1.5	1.6799 (1, 2, 7)	(0.5000, 0.9609) (1, 2, 4)	(0.5000, 0.9612) (1, 2, 4)
	2.0	1.6799 (1, 1, 3)	(0.5000, 0.9609) (1, 1, 2)	(0.5000, 0.9612) (1, 1, 2)
7	0.1	1.4372 (22, 298, 1285)	(0.1000, 0.2992) (16, 99, 393)	(0.1000, 0.2996) (13, 98, 395)
	0.2	1.4372 (14, 181, 779)	(0.1000, 0.2992) (9, 32, 104)	(0.1000, 0.2996) (7, 32, 104)
	0.4	1.4372 (5, 57, 247)	(0.1250, 0.3430) (5, 11, 27)	(0.1250, 0.3437) (4, 11, 27)
	0.6	1.4372 (2, 20, 87)	(0.2501, 0.5249) (3, 6, 14)	(0.2500, 0.5246) (3, 6, 14)
	0.8	1.4372 (1, 9, 35)	(0.5001, 0.8226) (2, 4, 11)	(0.5000, 0.8224) (2, 4, 11)
	1.0	1.4372 (1, 4, 17)	(0.5000, 0.8225) (1, 3, 6)	(0.5000, 0.8227) (1, 3, 6)
	1.5	1.4372 (1, 1, 4)	(0.7500, 1.1114) (1, 1, 3)	(0.7500, 1.1114) (1, 1, 3)
	2.0	1.4372 (1, 1, 2)	(0.7500, 1.1113) (1, 1, 2)	(0.7600, 1.1234) (1, 1, 2)
9	0.1	1.2755 (21, 282, 1217)	(0.1001, 0.2660) (15, 83, 322)	(0.1000, 0.2662) (12, 82, 323)
	0.2	1.2755 (12, 156, 672)	(0.1001, 0.2660) (8, 26, 81)	(0.1000, 0.2662) (7, 26, 81)
	0.4	1.2755 (4, 43, 186)	(0.1250, 0.3047) (4, 9, 21)	(0.1250, 0.3053) (3, 9, 21)
	0.6	1.2755 (2, 14, 61)	(0.2501, 0.4662) (2, 5, 11)	(0.2500, 0.4659) (2, 5, 11)
	0.8	1.2755 (1, 6, 24)	(0.5001, 0.7303) (1, 3, 8)	(0.5000, 0.7301) (1, 3, 8)
	1.0	1.2755 (1, 3, 11)	(0.5000, 0.7302) (1, 2, 5)	(0.5000, 0.7304) (1, 2, 5)
	1.5	1.2755 (1, 1, 3)	(0.5000, 0.7302) (1, 1, 2)	(0.5000, 0.7304) (1, 1, 2)
	2.0	1.2755 (1, 1, 1)	(0.5000, 0.7302) (1, 1, 2)	(0.5000, 0.7015) (1, 1, 2)
11	0.1	1.1581 (20, 268, 1155)	(0.1001, 0.2417) (14, 71, 271)	(0.1000, 0.2418) (11, 70, 271)
	0.2	1.1581 (11, 136, 587)	(0.1001, 0.2417) (8, 23, 66)	(0.1000, 0.2418) (6, 22, 66)
	0.4	1.1581 (3, 34, 146)	(0.2500, 0.4235) (3, 8, 22)	(0.2500, 0.4238) (3, 8, 22)
	0.6	1.1581 (1, 11, 45)	(0.2501, 0.4236) (2, 4, 9)	(0.2500, 0.4233) (2, 4, 9)
	0.8	1.1581 (1, 4, 17)	(0.5001, 0.6633) (1, 3, 6)	(0.5000, 0.6631) (1, 3, 6)
	1.0	1.1581 (1, 2, 8)	(0.5000, 0.6632) (1, 2, 4)	(0.5000, 0.6634) (1, 2, 4)
	1.5	1.1581 (1, 1, 2)	(0.5000, 0.6632) (1, 1, 2)	(0.5000, 0.6634) (1, 1, 2)
	2.0	1.1581 (1, 1, 1)	(0.7500, 0.8957) (1, 1, 1)	(0.7600, 0.9055) (1, 1, 1)

Table 5. Comparisons of the EMRL_1 and $(\ell_{0.05}, \mathrm{MRL}_1, \ell_{0.95})$ values for the Case-K Shewhart $\tilde{X}$ and optimal Case-K EWMA $\tilde{X}$ charts, together with the charts' corresponding parameters when $n \in \{3,5,7,9,11\}$, $\mathrm{EMRL}_0 = 370$, $\delta_{\min} = 0.1$ and $\delta_{\max} = 2.0$.

		Shewhart $\tilde{X}$	EWMA $\tilde{X}$ (Zero-state)	EWMA $\tilde{X}$ (Steady-state)
		L, EMRL_1	(λ, K) EMRL_1	(λ, K) EMRL_1
n	δ	$(\ell_{0.05}, \mathrm{MRL}_1, \ell_{0.95})$	$(\ell_{0.05}, \mathrm{MRL}_1, \ell_{0.95})$	$(\ell_{0.05}, \mathrm{MRL}_1, \ell_{0.95})$
		2.1022, 51.85	(0.1027, 0.4443) 13.85	(0.1008, 0.4396) 13.67
	0.1	(25, 333, 1438)	(21, 165, 681)	(17, 162, 680)
	0.2	(19, 253, 1092)	(13, 61, 228)	(10, 59, 226)
	0.4	(9, 119, 512)	(7, 20, 54)	(6, 19, 54)
3	0.6	(5, 55, 234)	(5, 11, 24)	(4, 11, 24)
	0.8	(2, 27, 114)	(4, 8, 15)	(3, 8, 15)
	1.0	(2, 14, 59)	(3, 6, 10)	(2, 6, 11)
	1.5	(1, 4, 15)	(2, 4, 6)	(2, 4, 6)
	2.0	(1, 2, 6)	(2, 3, 4)	(1, 3, 4)
		1.6799, 38.33	(0.1042, 0.3583) 10.14	(0.1042, 0.3592) 10.00
	0.1	(24, 315, 1359)	(18, 126, 509)	(15, 125, 513)
	0.2	(16, 212, 915)	(10, 42, 147)	(9, 41, 147)
	0.4	(6, 80, 344)	(6, 14, 35)	(5, 14, 35)
5	0.6	(3,32,135)	(4, 8, 16)	(4, 8, 16)
	0.8	(1,14,59)	(3, 6, 10)	(3, 6, 10)
	1.0	(1, 7,28)	(3, 5, 7)	(2, 5, 8)
	1.5	(1, 2, 7)	(2, 3, 4)	(2, 3, 5)
	2.0	(1, 1, 3)	(2, 2, 3)	(1, 2, 3)
		1.4372, 30.60	(0.1271, 0.3466) 8.35	(0.1281, 0.3489) 8.35
	0.1	(22, 298, 1285)	(16, 110, 445)	(13, 109, 450)
	0.2	(14, 181, 779)	(9, 34, 119)	(7, 34, 120)
	0.4	(5, 57, 247)	(5, 11, 27)	(4, 11, 27)
7	0.6	(1, 10, 42)	(3, 6,13)	(3, 7, 13)
	0.8	(1, 5, 19)	(3, 5, 8)	(3, 5, 8)
	1.0	(1, 4, 17)	(2, 4, 6)	(2, 4, 6)
	1.5	(1, 1, 4)	(2, 2, 3)	(1, 2, 4)
	2.0	(1, 1, 2)	(1, 2, 2)	(1, 2, 3)
		1.2755, 25.29	(0.1828, 0.3844) 7.56	(0.1828, 0.3849) 7.52
	0.1	(21, 282, 1217)	(13, 110, 452)	(12, 109, 455)
	0.2	(12, 156, 672)	(7, 32, 116)	(6, 31, 116)
	0.4	(4, 43, 186)	(4, 9, 24)	(3, 9, 24)
9	0.6	(1, 7, 28)	(3, 5, 11)	(3, 5, 11)
	0.8	(1, 6,24)	(2, 4, 6)	(2, 4, 6)
	1.0	(1, 3, 11)	(2, 3, 5)	(1, 3, 5)
	1.5	(1, 1, 3)	(1, 2, 3)	(1, 2, 3)
	2.0	(1, 1, 1)	(1, 2, 2)	(1, 2, 2)
		1.1581, 21.64	(0.2238, 0.3955) 6.63	(0.2258, 0.3980) 6.63
	0.1	(20, 268, 1155)	(13, 106, 439)	(11, 106, 443)
	0.2	(11, 136, 587)	(6, 29, 108)	(6, 29, 109)
	0.4	(3, 34, 146)	(3, 8, 21)	(3, 8, 21)
11	0.6	(1,11, 45)	(2, 5, 9)	(2, 5, 9)
	0.8	(1, 4,17)	(2, 3, 6)	(2, 3, 6)
	1.0	(1, 2, 8)	(2, 2, 4)	(1, 2, 4)
	1.5	(1, 1, 2)	(1, 2, 2)	(1, 2, 3)
	2.0	(1, 1, 1)	(1, 1, 2)	(1, 1, 2)

Table 6. The $(\ell_{0.05}, \mathrm{MRL}_1, \ell_{0.95})$ values for the optimal Case-U EWMA $\tilde{X}$ chart under zero-state, together with the chart's corresponding optimal parameters, (λ, K) when $n \in \{3, 5, 7, 9, \}, \delta_{\mathrm{opt}} \in \{0.1, 0.2, 0.4, 0.6, 0.8, 1.0, 1.5, 2.0\}$ and $\mathrm{MRL}_0 = 370$.

n	δ	10	20	40	80	100000
3	0.1	(0.1026, 0.5630) (15, 292, 30990)	(0.1007, 0.5150) (19, 268, 6783)	(0.1007, 0.4860) (19, 238, 2787)	(0.1006, 0.4668) (20, 211, 1658)	(0.1006, 0.4381) (21, 164, 674)
	0.2	(0.1026, 0.5630) (12, 155, 18800)	(0.1007, 0.5150) (13, 117, 3985)	(0.1026, 0.4913) (13, 92, 1327)	(0.1006, 0.4668) (13, 77, 611)	(0.1006, 0.4381) (13, 60, 225)
	0.4	(0.1104, 0.5840) (7, 37, 2758)	(0.1104, 0.5407) (8, 29, 407)	(0.1260, 0.5503) (7, 25, 154)	(0.1260, 0.5310) (7, 23, 95)	(0.1260, 0.5030) (7, 20, 59)
	0.6	(0.1260, 0.6227) (5, 16, 249)	(0.1260, 0.5796) (5, 14, 68)	(0.2510, 0.8126) (4, 13, 63)	(0.2510, 0.7937) (4, 12, 47)	(0.2510, 0.7683) (4, 11, 35)
	0.8	(0.2197, 0.8262) (3, 9, 76)	(0.2510, 0.8422) (3, 8, 37)	(0.2510, 0.8126) (3, 8, 25)	(0.2510, 0.7937) (3, 7, 21)	(0.2510, 0.7683) (3, 7, 18)
	1	(0.2510, 0.8865) (3, 6, 30)	(0.5010, 1.2727) (2, 6, 34)	(0.2510, 0.8126) (3, 5, 14)	(0.2510, 0.7937) (2, 5, 12)	(0.5010, 1.2038) (2, 5, 17)
	1.5	(0.5010, 1.3176) (1, 3, 12)	(0.7510, 1.692) (1, 3, 14)	(0.5010, 1.2437) (1, 3, 7)	(0.5010, 1.2259) (1, 3, 6)	(0.5010, 1.2038) (2, 5, 17)
	2	(0.5010, 1.3176) (1, 2, 5)	(0.5010, 1.2727) (1, 2, 4)	(0.5010, 1.2542) (1, 2, 4)	(0.5010, 1.2259) (1, 2, 4)	(0.5010, 1.2038) (1, 3, 6)
5	0.1	(0.1261, 0.4960) (14, 272, 13376)	(0.1026, 0.415) (18, 227, 4482)	(0.1007, 0.3880) (19, 190, 2242)	(0.1006, 0.3730) (19, 163, 1312)	(0.1006, 0.3503) (18, 124, 500)
	0.2	(0.1026, 0.4500) (8, 105, 10110)	(0.1007, 0.4110) (12, 75, 1876)	(0.1026, 0.3923) (12, 60, 679)	(0.1006, 0.3730) (11, 51, 322)	(0.1006, 0.3503) (11, 41, 144)
	0.4	(0.1261, 0.4960) (6, 23, 626)	(0.1260, 0.4622) (6, 19, 135)	(0.1260, 0.4393) (6, 17, 68)	(0.1260, 0.4242) (6, 16, 50)	(0.1260, 0.4021) (6, 14, 37)
	0.6	(0.2510, 0.7055) (3, 11, 96)	(0.2510, 0.6714) (3, 9, 42)	(0.2510, 0.6486) (3, 9, 29)	(0.2510, 0.6339) (3, 8, 24)	(0.2510, 0.6142) (3, 8, 20)
	0.8	(0.2510, 0.7055) (3, 6, 26)	(0.5010, 1.0144) (2, 6, 29)	(0.2510, 0.6486) (3, 5, 13)	(0.2510, 0.6339) (2, 5, 12)	(0.5010, 0.9622) (2, 5, 17)
	1	(0.5010, 1.0487) (2, 4, 20)	(0.5010, 1.0144) (2, 4, 13)	(0.5011, 0.9920) (2, 4, 11)	(0.5010, 0.9786) (2, 4, 10)	(0.5010, 0.9622) (2, 4, 9)
	1.5	(0.5011, 1.0490) (1, 2, 5)	(0.5010, 1.014) (1, 2, 4)	(0.5010, 0.9922) (1, 2, 4)	(0.5010, 0.9786) (1, 2, 4)	(0.5010, 0.9622) (1, 2, 4)
	2	(0.7510, 1.3818) (1, 1, 3)	(0.7510, 1.3481) (1, 1, 3)	(0.5010, 1.0002) (1, 1, 2)	(0.5010, 0.9786) (1, 1, 2)	(0.5010, 0.9622) (1, 1, 2)
7	0.1	(0.1261, 0.4250) (14, 246, 9848)	(0.1026, 0.3550) (16, 192, 3646)	(0.1007, 0.3320) (17, 155, 1837)	(0.1007, 0.3200) (17, 131, 1070)	(0.1007, 0.3000) (16, 99, 392)
	0.2	(0.1026, 0.385) (10, 54, 5882)	(0.1026, 0.355) (10, 54, 1249)	(0.1026, 0.3358) (10, 44, 398)	(0.1104, 0.3370) (10, 39, 213)	(0.1026, 0.3040) (10, 32, 109)
	0.4	(0.1260, 0.4248) (6, 17, 222)	(0.1572, 0.4448) (5, 14, 78)	(0.1260, 0.3761) (5, 13, 42)	(0.1260, 0.3632) (5, 12, 34)	(0.1261, 0.3450) (5, 11, 27)
	0.6	(0.2510, 0.6031) (3, 8, 42)	(0.2510, 0.5743) (3, 7, 24)	(0.2510, 0.5550) (3, 7, 19)	(0.2510, 0.5426) (3, 6, 16)	(0.2510, 0.5259) (3, 6, 14)
	0.8	(0.5010, 0.8961) (2, 5, 24)	(0.3760, 0.7256) (2, 4, 13)	(0.5010, 0.8486) (2, 4, 13)	(0.5010, 0.8373) (2, 4, 12)	(0.5010, 0.8235) (2, 4, 11)
	1	(0.5010, 0.8961) (1, 3, 10)	(0.5010, 0.8673) (1, 3, 8)	(0.5010, 0.8486) (1, 3, 7)	(0.5010, 0.8373) (1, 3, 7)	(0.5010, 0.8235) (1, 3, 6)
	1.5	(0.5010, 0.8961) (1, 2, 4)	(0.751, 1.152) (1, 2, 4)	(0.5010, 0.8486) (1, 2, 3)	(0.7510, 1.1243) (1, 1, 3)	(0.7510, 1.1125) (1, 1, 3)
	2	(0.5010, 0.8961) (1, 1, 2)	(0.5010, 0.8673) (1, 1, 2)	(0.5010, 0.8553) (1, 1, 2)	(0.5000, 0.8235) (1, 1, 2)	(0.5000, 0.8225) (1, 1, 2)
9	0.1	(0.1026, 0.3420) (14, 219, 7900)	(0.1016, 0.3140) (16, 163, 3333)	(0.1182, 0.3220) (15, 135, 1637)	(0.1006, 0.2837) (16, 108, 867)	(0.1006, 0.2660) (15, 83, 333)
	0.2	(0.1026, 0.3420) (10, 57, 3856)	(0.1026, 0.3156) (10, 42, 767)	(0.1182, 0.3220) (9, 36, 273)	(0.1026, 0.2868) (9, 31, 144)	(0.1006, 0.2660) (8, 26, 81)
	0.4	(0.2510, 0.5352) (4, 14, 168)	(0.2510, 0.5098) (4, 12, 66)	(0.2510, 0.4928) (4, 11, 43)	(0.2510, 0.4818) (4, 10, 35)	(0.2510, 0.4670) (3, 10, 28)
	0.6	(0.2510, 0.5352) (3, 6, 25)	(0.5010, 0.7696) (2, 6, 29)	(0.5010, 0.7532) (2, 6, 22)	(0.2510, 0.4818) (3, 5, 12)	(0.2510, 0.4670) (2, 5, 11)
	0.8	(0.5010, 0.7948) (2, 4, 15)	(0.5010, 0.7696) (2, 4, 11)	(0.5010, 0.7532) (2, 3, 9)	(0.5010, 0.7432) (2, 3, 9)	(0.5010, 0.7312) (1, 3, 8)
	1	(0.5010, 0.7948) (1, 3, 7)	(0.5010, 0.7696) (1, 3, 6)	(0.5010, 0.7532) (1, 2, 5)	(0.5010, 0.7432) (1, 2, 5)	(0.5010, 0.7312) (1, 2, 5)
	1.5	(0.7510, 1.0467) (1, 1, 3)	(0.7510, 1.0220) (1, 1, 3)	(0.7510, 1.0066) (1, 1, 3)	(0.5010, 0.7432) (1, 1, 2)	(0.5010, 0.7312) (1, 1, 2)
	2	(0.5010, 0.7948) (1, 1, 2)	(0.5010, 0.7696) (1, 1, 2)	(0.5010, 0.7591) (1, 1, 2)	(0.5000, 0.7301) (1, 1, 2)	(0.5000, 0.7302) (1, 1, 2)

Table 7. Phase I dataset for illustrative example of the optimal EWMA $\tilde{X}$ chart based on EMRL.

i	Phase I ($X_{i,j}$)					$\tilde{X}_i$	R_i
1	74.030	74.002	74.019	73.992	74.008	74.008	0.038
2	73.995	73.992	74.001	74.011	74.004	74.001	0.019
3	73.988	74.024	74.021	74.005	74.002	74.005	0.036
4	74.002	73.996	73.993	74.015	74.009	74.002	0.022
5	73.992	74.007	74.015	73.989	74.014	74.007	0.026
6	74.009	73.994	73.997	73.985	73.993	73.994	0.024
7	73.995	74.006	73.994	74.000	74.005	74.000	0.012
8	73.985	74.003	73.993	74.015	73.988	73.993	0.030
9	74.008	73.995	74.009	74.005	74.004	74.005	0.014
10	73.998	74.000	73.990	74.007	73.995	73.998	0.017
11	73.994	73.998	73.994	73.995	73.990	73.994	0.008
12	74.004	74.000	74.007	74.000	73.996	74.000	0.011
13	73.983	74.002	73.998	73.997	74.012	73.998	0.029
14	74.006	73.967	73.994	74.000	73.984	73.994	0.039
15	74.012	74.014	73.998	73.999	74.007	74.007	0.016
16	74.000	73.984	74.005	73.998	73.996	73.998	0.021
17	73.994	74.012	73.986	74.005	74.007	74.005	0.026
18	74.006	74.010	74.018	74.003	74.000	74.006	0.018
19	73.984	74.002	74.003	74.005	73.997	74.002	0.021
20	74.000	74.010	74.013	74.020	74.003	74.010	0.020
21	73.982	74.001	74.015	74.005	73.996	74.001	0.033
22	74.004	73.999	73.990	74.006	74.009	74.004	0.019
23	74.010	73.989	73.990	74.009	74.014	74.009	0.025
24	74.015	74.008	73.993	74.000	74.010	74.008	0.022
25	73.982	73.984	73.995	74.017	74.013	73.995	0.035

Table 8. Phase II dataset for illustrative example of the optimal EWMA $\tilde{X}$ chart based on EMRL.

i	Phase II ($Y_{i,j}$)					$\tilde{Y}_i$	Z_i
1	74.012	74.015	74.030	73.986	74.000	74.012	74.005
2	73.995	74.010	73.990	74.015	74.001	74.001	74.004
3	73.987	73.999	73.985	74.000	73.990	73.990	74.001
4	74.008	74.010	74.003	73.991	74.006	74.006	74.002
5	74.003	74.000	74.001	73.986	73.997	74.000	74.001
6	73.994	74.003	74.015	74.020	74.004	74.004	74.002
7	74.008	74.002	74.018	73.995	74.005	74.005	74.003
8	74.001	74.004	73.990	73.996	73.998	73.998	74.002
9	74.015	74.000	74.016	74.025	74.000	74.015	74.005
10	74.030	74.005	74.000	74.016	74.012	74.012	**74.007**
11	74.001	73.990	73.995	74.010	74.024	74.001	74.005
12	74.015	74.020	74.024	74.005	74.019	74.019	**74.009**
13	74.035	74.010	74.012	74.015	74.026	74.015	**74.010**
14	74.017	74.013	74.036	74.025	74.026	74.025	**74.014**
15	74.010	74.005	74.029	74.000	74.020	74.010	**74.013**

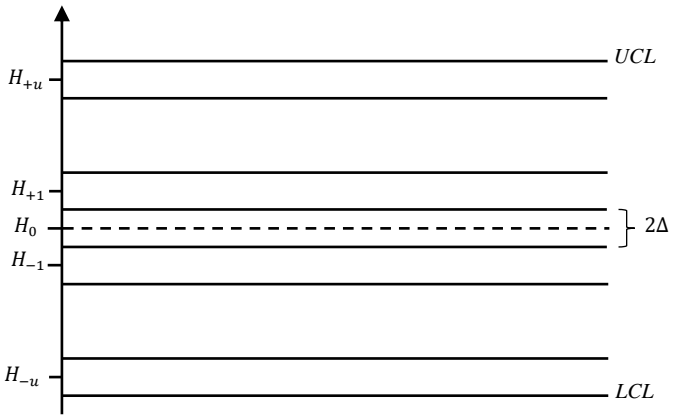

Figure 1. Interval between lower and upper control limits divided into $2u + 1$ subintervals of width 2Δ each.

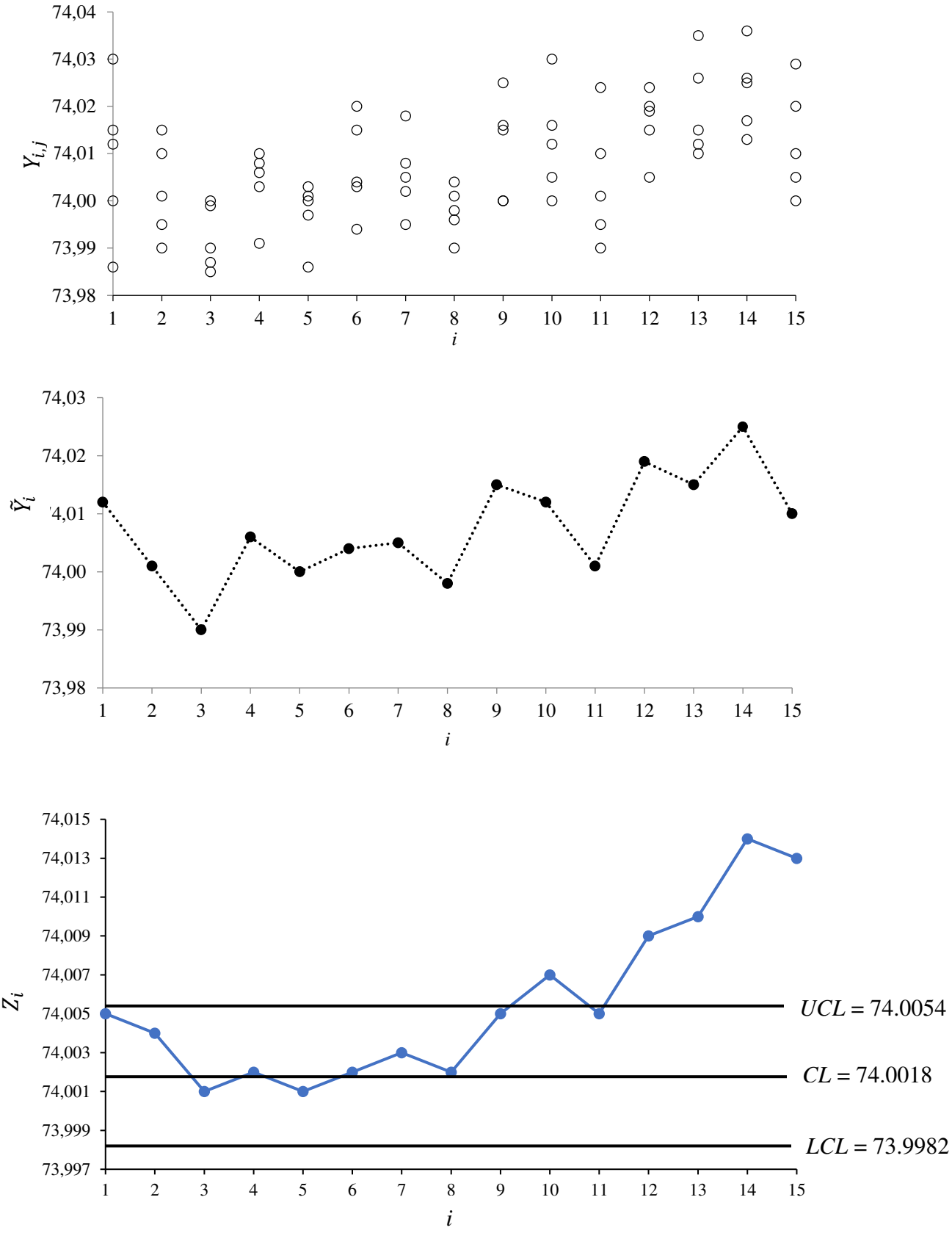

Figure 2. EWMA $\tilde{X}$ chart corresponding to the Phase II dataset in Table 8.